Pergamon

Geochimica et Cosmochimica Acta, Vol. 61, No. 13, pp. 2731–2747, 1997

0016-7037/97 $17.00 + .00

PII S0016-7037(97)00082-3

Anatexis of lunar cumulate mantle in time and space: Clues from trace-element, strontium, and neodymium isotopic chemistry of parental Apollo 12 basalts

Gregory A. Snyder,[1] Clive R. Neal,[2] Lawrence A. Taylor,[1] and Alex N. Halliday[3]

[1]Planetary Geosciences Institute, Department of Geological Sciences, University of Tennessee, Knoxville, Tennessee 37996, USA
[2]Department of Civil Engineering and Geological Sciences, University of Notre Dame, South Bend, Indiana 46556, USA
[3]Department of Geological Sciences, University of Michigan, Ann Arbor, Michigan 48109, USA

(*Received October* 15, 1996; *accepted in revised form February* 10, 1997)

Abstract—In an effort to elucidate the processes of lunar mantle melting, and the magma evolution of mare basalts within Oceanus Procellarum on the western lunar near-side, we have analyzed seven fine-grained to vitrophyric Apollo 12 basalts for trace-elements; five of these also have been analyzed for Nd and Sr isotopic compositions. These samples represent all three main groups identified among the Apollo 12 mare basalts and have been proposed as parental melts to their respective groups, i.e., olivine-, pigeonite-, and ilmenite-basalts. The sources for these low-Ti mare basalts are postulated to have formed from crystallization of a global magma ocean. Li-Be systematics, combined with REE data, indicate that the specific sources for the Apollo 12 low-Ti mare basalts were generated after 82–94% crystallization of this lunar magma ocean. In fact, it seems that all mare basalts analyzed from the Apollo collections were generated from cumulates precipitated in the last 20% of the magma ocean. Chemical compositions of fine-grained pigeonite and olivine basalts are consistent with 7–9% nonmodal (in proportions not defined by experimental petrology and phase equilibria) melting of a source consisting of 48% olivine, 30% calcic clinopyroxene, and 22% pigeonite (as per Neal et al., 1994b). Sm-Nd and Rb-Sr abundance data also suggest that the pigeonite- and olivine-basalt source contained from 0.3 to 0.5% trapped residual liquid from the magma ocean. The compositions of the two fine-grained ilmenite basalts are consistent with 5–7% partial melting of a source with subequal proportions of olivine (45.5%) and pigeonite (42.5%) and lesser amounts of clinopyroxene (11.5%) and entrained plagioclase (0.5%). Furthermore, the ilmenite source was nearly devoid of trapped liquid (<0.15%). A few of these samples do indicate minor post-extrusive fractionation, but most of the samples are considered to be unfractionated, primitive magmas that are parental to the other mare basalts.

Isotopic systematics of the Apollo 12, fine-grained, parental basalts are consistent with their derivation from two distinct mantle source regions. Both of these sources were LREE depleted for extended periods of time: up to 600 million years for the ilmenite-basalt source and up to 900 million years for the pigeonite- and olivine-basalt source. Due in part to the relatively small proportion of low Sm/Nd, trapped, residual magma-ocean liquid in the source (<0.15%), the Nd isotopic compositions of the ilmenite basalts are among the most radiogenic ever analyzed from the Moon (ϵ_{Nd} = +10.5 to +11.2, at 3.2 Ga). The mantle source for the olivine and pigeonite basalts contained a higher proportion of trapped, residual, magma-ocean liquid (0.3 to 0.5%), thus yielding less radiogenic Nd isotopic signatures (ϵ_{Nd} = +4.3 to +4.7, at 3.2 Ga).

By integrating this information on parental, low-Ti, Apollo 12 basalts with mare basalt and picritic glass data from other landing sites, as well as telescopic and remote-sensing data, we propose a model for melting of the lunar interior. The upper 400–500 km of the lunar mantle is a consequence of incipient melting of the Moon and formation of a global magma ocean. This magma ocean became progressively enriched in incompatible elements as it precipitated the cumulate upper mantle. This incompatible-element enriched liquid was also trapped in varying proportions in the differentiated cumulates. The earliest, extensive mare magmas (high-Ti mare basalts) were generated at shallow depths in the mantle from cumulate source-regions that had trapped relatively large proportions of this incompatible-element enriched, residual, magma ocean liquid. These source regions also contained the late-crystallizing phase ilmenite and, thus, generated high-Ti magmas. The trapped liquid component contained elevated abundances of heat-producing elements (K, U, and Th), increasing the fertility of associated source-regions. With time, melting moved progressively deeper in the mantle to source-regions with less of the residual, heat-producing, magma ocean liquid. Due to density contrasts, the ilmenite-bearing upper portions of the lunar mantle sank into the cumulate pile, possibly carrying more fertile material with it and allowing melting of more Mg-enriched source regions (to form the high-Ti picritic glass beads). Thus, the major controlling factors in the melting of the lunar interior could be the proportion of trapped, magma-ocean liquid in the cumulate source and the sinking of more fertile, ilmenite-bearing material into the lower mantle.

1. INTRODUCTION

Understanding the production and evolution of mare basalts is paramount to constructing a more complete picture of the composition and evolution of the Moon's mantle. Whereas most of our information about mare basalts is from samples collected at the Apollo 11, 15, and 17 landing sites on the eastern near-side, the Apollo 12 mare basalt suite from Oceanus Procellarum allows the only substantive look at basaltic volcanism on the western near-side of the Moon. Mare basalts collected from the Apollo 12 landing site in Oceanus Procellarum have been subdivided into three major types (Warner, 1971; James and Wright, 1972; Dungan and Brown, 1977; Rhodes et al., 1977; Neal et al., 1994a) based on petrography and confirmed by mineral chemistry: *olivine-*, *pigeonite*, and *ilmenite* basalts. A single sample, so-called "feldspathic" basalt 12038 (Beaty et al., 1979), is anomalous and may either be a separate basalt type at the Apollo 12 landing site, or not indigenous (Nyquist et al., 1979; Neal et al., 1994a).

The mineralogy and major- and trace-element chemical compositions of all Apollo 12 basalts led previous workers (Warner, 1971; Rhodes et al., 1977; Neal et al. 1994a,b) to propose parental compositions for each group. Based mostly upon major-element correlations, Neal et al (1994b) proposed that vitrophyre 12011 was parental to all other pigeonite basalts from the Apollo 12 landing site. In order to compensate for the removal and/or accumulation of olivine in derived samples, an average of three vitrophyric/quench-textured basalts (12008, 12022, and 12045) was used as the parental composition for the ilmenite-basalts (Neal et al., 1994b). A similar approach was taken to determine that an average of vitrophyric samples 12009 and 12015 was the most suitable parental composition for the olivine basalts.

Considerable isotopic work was previously conducted on the Apollo 12 mare basalts. Argon isotopic analyses were performed on most samples by a variety of analysts (e.g., Turner, 1971; Stettler et al., 1973; Alexander and Davis, 1974; Horn et al., 1975) and yielded ages of 3.1 to 3.3 Ga. Several groups also analyzed the Apollo 12 basalts for their Sr isotopic compositions and confirmed the ^{40}Ar-^{39}Ar ages with Rb-Sr mineral ages on a small group of samples (e.g., Papanastassiou and Wasserburg, 1970, 1971a; Compston et al., 1971). However, it was not until the work of Nyquist and coworkers (Nyquist et al.,1977; Nyquist et al., 1979; Nyquist et al., 1981) that a systematic study of all Apollo 12 basalt groups, including Rb-Sr and Sm-Nd isotopic and trace-element analyses, was undertaken with the goal of producing information on the character and timing of source formation and subsequent melting. They found that there were systematic differences between the ilmenite basalts and the olivine-pigeonite basalts that could be explained only by derivation from separate sources. However, they did not report Nd isotopic data for many of the samples considered to be parental to these basalts.

In an attempt to gain a better understanding of the low-Ti mantle sources of volcanism on the western lunar near-side, we have collected a full complement of trace-element data, as well as Nd isotopic data, on seven samples which represent near-liquid parental compositions for these three main basalt groups. With these samples, we may be able to "see through" surface processes, such as fractional crystallization, crystal accumulation, and crustal contamination, which have modified other basalts from the Apollo 12 landing site, to the original mantle sources of this important group of western near-side basalts. By combining this data on "primitive" low-Ti basalts with an understanding of the volcanic stratigraphy in Oceanus Procellarum, age information from the Apollo collections, and geochemical studies of other mare and picritic glasses, we will construct a plausible model of lunar mantle evolution and melting over time.

2. VOLCANIC STRATIGRAPHY IN OCEANUS PROCELLARUM

Oceanus Procellarum is the largest of the lunar maria spanning ~1.7 million km^2 of the lunar surface and containing volcanic flows with an estimated volume of 8.7×10^5 km^3 (Whitford-Stark and Head, 1980). The basin which contains these volcanics was created by one of the oldest preserved impact events on the Moon. This impact event is similar in age to that which formed the South Pole-Aitken basin and is estimated to have occurred between 4.1 and 4.2 Ga (Wilhelms, 1987).

Based upon telescopic observations, albedo variations, crater density studies (which, in concert with geochronologic and isotopic studies of Apollo samples, yield age information), and remote sensing, the basalts within Oceanus Procellarum have been subdivided into four major units and are (in order of decreasing age and increasing superposition): the Repsold, Telemann, Hermann, and Sharp Formations (Whitford-Stark and Head, 1980). The Repsold Formation is the oldest macro-unit with various individual flows having estimated ages of 3.7 to 3.8 Ga. The flows which make up this formation are Ti- and Th-rich (TiO_2 = 3–11 wt%, Th = 9 ppm) and some may be correlative with the high-Ti basalts collected at the Apollo 11 and 17 and Luna 16 landing sites on the eastern near-side (Whitford-Stark and Head, 1980).

The Telemann Formation overlays the Repsold Formation, was probably extruded between 3.4 and 3.8 Ga, and and is notably Ti and Th poor (TiO_2 < 2 wt%; Th = 2.5 ppm). Some of the volcanic units from the Telemann Formation may be correlative with very low-Ti (VLT) basalts collected at the Luna 24 landing site in Mare Crisium. The Telemann Formation is volumetrically the largest, making up nearly half of the volcanic pile although it covers only 1/10 of the surface in the Procellarum basin (Whitford-Stark and Head, 1980).

The Hermann Formation has the greatest areal extent of the four major volcanic units in the Procellarum basin (nearly one-half of the total areal exposure of basin-filling material) although volumetrically, it composes one-fourth of the total volcanic pile. This formation is composed of volcanic units which are intermediate in Ti contents (TiO_2 = 1–6 wt%), but low in Th, K, and U. The ages of these volcanic units are thought to be between 3.0 and 3.6 Ga and the Apollo 12 basalts were collected from this formation (Whitford-Stark and Head, 1980).

The uppermost Sharp Formation is thin, comprises only 2% of the total volcanic pile, but is areally extensive (~42% of the total area in the Procellarum basin). The chemistry determined from remote-sensing is somewhat surprising, as this formation contains high-Ti basalts similar to those of the much older Repsold Formation. Basalt flows from the Sharp formation are thought to have ages between 2.0 and 3.4 Ga (Pieters et al., 1980; Whitford-Stark and Head, 1980).

Thus, there is evidence in the volcanic stratigraphy for high-Ti basaltic volcanism in Oceanus Procellarum. Some of the high-Ti volcanic units in Oceanus Procellarum are similar in age to those in Mare Tranquillitatis and Mare Serenitatis and collected at the Apollo 11 and 17 landing sites, respectively. Furthermore, there is evidence

for a much later high-Ti volcanic event at 2.5 ± 0.5 Ga (Pieters et al., 1980). An important part of any lunar-mantle melting model must include provisions for two major pulses, separated in time, of high-Ti basaltic volcanism: one pulse at 3.56 to 3.85 Ga (Nyquist and Shih, 1992; Snyder et al., 1994; Snyder et al., 1996) and another at 2.5 ± 0.5 Ga (Pieters et al., 1980). Flows from these two separate high-Ti volcanic events do not occur near the surface at the Apollo 12 landing site and, therefore, were not sampled. However, high-Ti picritic glass beads, representative of pyroclastic, fire-fountain activity, have been sampled from the Apollo 12 landing site (Delano, 1986).

3. ANALYTICAL METHODS AND DATA PRESENTATION CONVENTIONS

Trace-elements were analyzed with a FISONS-VG PlasmaQuad II STE Inductively Coupled Plasma Mass Spectrometer (ICP-MS) at the University of Notre Dame. The facility is housed in a class 1000 clean lab kept under positive pressure as is a class 1000 clean lab which is also available for sample preparation. Splits of samples for ICP-MS analysis were crushed in acetone in an agate mortar before being dissolved using standard HF/HNO_3 techniques on a hot plate at 150°C. The resulting solution was evaporated and the residue treated with two 1–2 mL washes of concentrated HNO_3 before being dissolved and analyzed in 2% HNO_3. All acids used were double-distilled, resulting in a full procedural blank generally at the sub-ppt (parts per trillion) level. External calibration procedures were used to quantify elements in the unknowns, and these were prepared from SPEX® liquid standards. Internal standards used were As (as the matrix contained no Cl^- and, hence, no ArCl interference on mass 75), Te, and In. All standards were run as unknowns in order to check calibrations, and blanks were periodically run to check for memory effects, which were minimal at worst. Machine detection limits are less than 10 ppt, except for Cr (597 ppt) and Ni (367 ppt). Relative errors, on the basis of five repeats, are indicated for each element at the 2-sigma level in Table 1.

At the University of Michigan, ~1 g samples were crushed in acetone in a boron carbide mortar under a flow of better than class 100 air. The full sample was mixed and quartered until a representative 50–70 mg split was attained. This split was then dissolved in HF, HNO_3, and HCl and isotope dilution measurements made on a 10–15% split of this solution with ^{87}Rb-^{84}Sr and ^{149}Sm-^{150}Nd mixed spikes. Rubidium-strontium isotopic systematics were not determined on 12009,126. Due to an analytical problem, Rb and Sr abundances for sample 12015,24 were not determined by isotope dilution; data in Table 3 for this sample are taken from ICP-MS data. Total-process blanks for chemical procedures were always less than 10 pg Rb, 120 pg Sr, 10 pg Sm, and 50 pg Nd. Sr and Nd isotopic data were obtained by multidynamic analysis on a VG Sector multicollector mass spectrometer. All Sr and Nd isotopic analyses are normalized to $^{86}Sr/^{88}Sr = 0.1194$ and $^{146}Nd/^{144}Nd = 0.7219$, respectively. Analyses of SRM 987 Sr and La Jolla Nd standards were performed throughout this study and gave weighted averages (at the 95% confidence limit, external precision) of $^{87}Sr/^{86}Sr = 0.710250 \pm 0.000011$ and $^{143}Nd/^{144}Nd = 0.511854 \pm 0.000011$, respectively. Internal, within-run, statistics are almost always of higher precision than the external errors (see Table 2 for within-run statistics of samples which are comparable to that of the standards). All isotope dilution measurements utilized static mode multicollector analyses.

By convention, the Nd isotopic data are also presented in Table 2 in epsilon units, deviation relative to a chondritic uniform reservoir, CHUR (DePaolo and Wasserburg, 1976):

$$\epsilon_{Nd} = [(^{143}Nd/^{144}Nd_{sample} - {}^{143}Nd/^{144}Nd_{CHUR})/{}^{143}Nd/^{144}Nd_{CHUR}] \times 10^4 \quad (1)$$

where present-day $(^{143}Nd/^{144}Nd)_{CHUR} = 0.512638$. Model ages (or single-stage evolution ages) have been calculated for both Nd and Sr isotopes and are given under the headings T_{LUNI} and T_{LUM}, respectively, in Table 2, where,

$$T_{LUNI} = 1/\lambda \times \ln[((^{87}Sr/^{86}Sr - 0.69903)/{}^{87}Rb/^{86}Sr) + 1] \quad (2)$$

and,

$$T_{LUM} = 1/\lambda \times \ln[(^{143}Nd/^{144}Nd - 0.516149)/(^{147}Sm/^{144}Nd - 0.318) + 1] \quad (3)$$

The T_{LUNI} model age is determined relative to a suggested lunar initial $^{87}Sr/^{86}Sr = LUNI = 0.69903$ at 4.55 Ga (Nyquist et al., 1973). The value for T_{LUM} yields a model age at which the sample was in equilibrium with a Lunar Upper Mantle (LUM) with a $^{147}Sm/^{144}Nd = 0.318$ (Snyder et al., 1994) and which has a present-day $^{143}Nd/^{144}Nd = 0.516149$. This model LUM is considered to be the *most*-depleted upper mantle and, thus, yields maximum ages for separation from an adcumulate lunar upper mantle (Snyder et al., 1994). This lunar adcumulate source was formed late in the crystallization of a lunar magma ocean (Snyder et al., 1992). Errors in the model ages are estimated from consideration of errors in the parent-daughter ratios and measured isotopic ratios.

4. PETROGRAPHY AND MINERAL CHEMISTRY

The petrography and mineral chemistry of all three groups of Apollo 12 basalts have been studied in detail, and only a summary of previous findings will be given here. Some of the earliest studies of Apollo 12 mare basalts subdivided them based upon petrography and mineral chemistry (Warner, 1971; James and Wright, 1972; Dungan and Brown, 1977; Rhodes et al., 1977). For the most part, these subdivisions have been upheld, and these original three groups are currently considered: pigeonite, olivine, and ilmenite basalts.

4.1. Olivine Basalts

The three olivine basalts (12009, 12015, and 12072) have the highest (12009 = 48.8%; 12015 = 62.3%) and lowest proportion of olivine (12072 = 5.7%) found in this group. Olivines occur as phenocrysts, with included FeNi grains and as skeletal microphenocrysts, indicative of rapid cooling. Baldridge et al. (1979) postulated that 12015 represented a "quenched liquid." Olivine compositions vary from Fo_{70} to Fo_{74} in cores to Fo_{59} to Fo_{67} in the rims. Both 12009 and 12015 contain substantial amounts of glass/mesostasis and are plagioclase-free, whereas 12072 is relatively glass-poor and plagioclase-rich (38.9 modal%; An_{89-91}). This high plagioclase content in 12072, along with a major-element "modal reconstruction" from mineral chemistry, originally led to its classification as a "feldspathic basalt" (Beaty et al., 1979). However, based on major- and trace-element analyses, Neal et al (1994a) reclassified 12072 as an olivine basalt. Groundmass pyroxenes in 12072 are notably Ca-poor ($Wo_9En_{56}Fs_{35}$), whereas phenocrysts vary in composition from $Wo_{31}En_{42}Fs_{27}$ to more evolved $Wo_{16}En_3Fs_{81}$ (pyroxferroite). In contrast to other groups which are relatively chromite-poor, all samples of this suite contain from 1 to 3 modal% chromite-ulvöspinel. Tridymite is present along with small amounts of ilmenite.

4.2. Pigeonite Basalts

The two pigeonite basalts, 12011 and 12043, are fine grained, but contain only a small proportion of glass. Olivine occurs as equant, occasionally prismatic phenocrysts (~1 mm) of Fo_{62-70} composition in both fine-grained samples. These olivine phenocrysts commonly are embayed and partially overgrown by pyroxene. Sample 12011 contains the largest proportion of olivine (7.6 modal%) found in the pigeonite-basalts, is the finest grained sample of the suite, and is considered to be a quenched liquid (Baldridge et al., 1979). Pigeonite phenocrysts are rather large (up to 3–4 mm) and are mostly in the compositional range $Wo_{8-10}En_{54-49}Fs_{33-32}$. Groundmass pyroxenes are anhedral to acicular and finer-grained (typically 0.4–0.8 mm) and vary in composition from pigeonite to augite. Plagioclase is most abundant in the pigeonite basalts and varies from An_{77} to An_{88} in the fine-grained samples. Pigeonite basalts generally contain a significant proportion of silica (both tridymite and cristobalite) and a slightly larger modal% of ilmenite than the olivine basalts.

Table 1. Whole-rock chemistry of Apollo 12 fine-grained basalts.

Samp SubS Type	12009 ,126 olv	12015 ,24 olv	12072 ,9 olv	12011 26 pig	12043 ,11 pig	12022 ,268 ilm	12045 ,18 ilm	Ave. % error (2σ)
SiO_2	45.0	45.0	(48.2)	46.6	46.8	43.2	42.3	—
TiO_2	2.90	2.86	3.0	3.29	3.38	5.16	4.78	—
Al_2O_3	8.59	8.57	8.5	9.77	10.1	9.04	8.06	—
FeO	21.0	20.2	21.3	19.5	19.5	21.4	22.1	—
MnO	0.28	0.29	0.26	0.29	0.29	0.25	0.29	—
MgO	11.6	11.9	13.3	8.26	7.68	10.4	11.6	—
CaO	9.42	9.21	8.7	10.6	11.0	9.56	9.09	—
Na_2O	0.23	0.23	0.23	0.25	0.27	0.47	0.26	—
K_2O	0.06	0.06	0.06	0.06	0.06	0.07	0.07	—
P_2O_5	0.07	0.06	—	0.07	0.06	0.13	0.09	—
Cr_2O_3	0.55	0.68	0.55	0.59	0.50	0.56	0.59	—
Mg#	50	51	53	43	41	46	48	—
Li (ppm)	6.7	7.6	6.0	8.5	11	9.1	8.5	4
Be	0.18	0.61	0.32	—	0.43	0.81	0.51	10
Sc	(46)*	(47)	(47)	(52)	(52)	(55)	(54)	
Cr	3960	2470	3820	2510	2270	3300	3800	15
Co	50.1	51.9	48.2	47.7	36.4	52.6	55.9	3
Ni	55.0	73.5	55.5	30.9	18.2	47.4	56.1	4
Cu	10.4	12.4	8.86	14.9	10.1	17.6	16.4	4
Zn	9.7	12.0	8.14	13.2	9.02	11.5	9.98	6
Ga	3.11	3.63	2.85	4.20	3.15	4.24	3.83	4
Rb	0.987	1.094	0.883	1.327	2.497	0.841	0.709	11
Sr	86.4	102.1	75.13	117.9	117.2	142.5	132.1	4
Y	36.5	34.5	30.7	38.4	42.1	64.2	49.7	3
Zr	106.4	127.6	95.9	(128)	125	160.1	109.9	3
Nb	6.5	8.01	5.36	—	6.85	7.04	5.17	3
Ag	0.082	0.218	0.107	0.191	0.150	0.105	0.398	18
Cs	0.068	0.078	0.047	0.072	0.159	0.058	0.038	15
Ba	55.5	67.0	51.2	79.1	69.2	58.4	52.9	3
La	5.62	6.00	6.23	7.77	6.00	6.50	6.65	4
Ce	16.1	16.7	17.0	18.5	16.2	17.9	17.3	3
Pr	2.45	2.70	2.22	2.79	2.58	3.35	2.83	4
Nd	12.7	16.1	11.0	14.2	13.6	19.2	15.1	4
Sm	3.91	4.77	4.01	4.80	5.15	6.58	5.64	5
Eu	0.89	1.07	0.85	1.11	0.93	1.45	1.06	5
Gd	4.15	6.10	3.91	5.22	5.47	7.94	6.04	6
Tb	0.90	1.10	0.74	0.94	1.03	1.66	1.26	6
Dy	5.70	6.98	4.52	5.87	6.65	10.39	7.74	4
Ho	1.14	1.50	0.97	1.32	1.42	2.10	1.60	5
Er	3.39	4.09	2.66	3.73	3.96	5.81	4.41	5
Tm	0.48	0.57	0.37	0.51	0.57	0.82	0.63	6
Yb	3.05	3.59	2.63	3.86	3.90	5.36	4.25	6
Lu	0.45	0.50	0.33	0.47	0.51	0.78	0.58	8
Ta	0.296	0.432	0.244	—	0.355	0.381	0.274	10
Hg	3.6	3.86	2.86	3.75	4.14	5.87	4.48	8
Pb	0.096	0.440	0.352	0.317	0.192	0.290	0.151	20
Th	0.850	0.680	0.726	0.415	0.850	0.987	0.679	15
U	0.230	0.330	0.164	0.291	0.258	0.280	0.176	20

* Values in parentheses are averages from other literature sources.

Major-element data sources: 12009, Compston et al. (1971); 12011, 12015, 12043, 12045, Rhodes et al. (1977); 12022, Engel et al. (1971); 12072, Neal et al. (1994a).

4.3. Ilmenite Basalts

Ilmenite basalts, by definition, contain substantial amounts of ilmenite (1.9–6.8 modal%), but also may have abundant olivine (up to 38.2 modal%; Neal et al., 1994a). Samples 12008 (not analyzed in this study), 12022, and 12045 represent the most rapidly cooled samples of this group (Dungan and Brown, 1977) and have ilmenite compositions that are the lowest in Cr_2O_3 (<0.2 wt%) and MgO (<0.5 wt%). Olivines in the fine-grained basalts are the most magnesian (Fo_{58-74} with most grains of Fo_{68-72} compositon; Dungan and Brown, 1977) and, unlike other samples of this suite, show no resorption features. Rims of olivines are generally up to 10–15 Fo units lower than the cores and may contain relatively Ni-rich FeNi metal. Augite phenocrysts ($Wo_{26-46}En_{49-29}Fs_{25-26}$) exhibit dendritic

Table 2: Rb-Sr and Sm-Nd Abundances and Isotopic Composition of Apollo 12 Fine-grained Basalts

Sample	Type	wt.(mg)	Rb (ppm)	Sr (ppm)	$^{87}Rb/^{86}Sr^{*}$	$^{87}Sr/^{86}Sr$	$^{87}Sr/^{86}Sr_i^{\#}$	$T_{LUNI}^{@}$	Sm (ppm)	Nd (ppm)	$^{147}Sm/^{144}Nd^{+}$	$^{143}Nd/^{144}Nd$	$\varepsilon_{Nd(T)}^{**}$	$T_{LUM}^{\&}$
12009,126	Oliv	52	1.05	98	0.0310	0.70096±5	0.69954±6	4.31	4.53	13.4	0.2046	0.513025±13	+4.3±0.4	4.15
12015,24	Oliv	53	1.09	102	0.0309	0.701017±13	0.699599±37	4.44	4.41	13.1	0.2036	0.513015±14	+4.5±0.4	4.13
12011,26	Pig	52	1.30	124	0.0302	0.700987±09	0.699584±17	4.48	5.27	15.8	0.2024	0.512995±16	+4.7±0.4	4.12
12022,268	Ilm	67	0.726	142	0.0147	0.700007±14	0.699324±16	4.59	5.64	15.1	0.2262	0.513797±24	+10.5±0.6	3.87
12045,18	Ilm	56	0.753	154	0.0140	0.699955±11	0.699202±13	4.56	6.10	16.2	0.2273	0.513854±21	+11.2±0.5	3.82

* Errors on this ratio are <1 % relative, except for 12015,24 where the error is estimated at 2%.
\# Initial $^{87}Sr/^{86}Sr$ are calculated at 3.2 Ga; Rb, Sr abundances and Sr isotopic data for 12009 from Papanastassiou and Wasserburg (1971a); Rb and Sr abundances for 12015,24 from ICP-MS data.
@ $T_{LUNI} = 1/\lambda \times \ln[((^{87}Sr/^{86}Sr - 0.69903)/^{87}Rb/^{86}Sr) + 1]$.
\+ Errors on this ratio are always <0.2% relative.
** ε_{Nd} calculated at 3.2 Ga.
& $T_{LUM} = 1/\lambda \times \ln[(^{143}Nd/^{144}Nd - 0.516149)/(^{147}Sm/^{144}Nd - 0.318) + 1]$. T_{LUM} yields a model age at which the sample was in equilibrium with a Lunar Upper Mantle with a $^{147}Sm/^{144}Nd = 0.318$ and which has a present-day $^{143}Nd/^{144}Nd = 0.516149$.

to elongate habits in the fine-grained basalts, again indicative of rapid cooling. Low-Ca rims on augite phenocrysts are common. Rare low-Ca phenocrysts have compositions of $Wo_{14-15}En_{61-56}Fs_{25-29}$ (Dungan and Brown, 1977). Plagioclase is similar in composition among the ilmenite basalts (An_{88-92} cores), but relatively depleted in the fine-grained samples. Spinels [Cr/(Cr+Al) = 0.66–0.74] are typically intergrown with late, Ni-poor, FeNi metal.

5. MAJOR- AND TRACE-ELEMENT COMPOSITIONS

The major-element compositions obtained from literature sources for these seven fine-grained to vitrophyric basalts are similar to those of the previously determined olivine, pigeonite, and ilmenite basalt groups (Table 1, Fig. 1). All seven basalts contain significant amounts of TiO_2 (i.e., 2.86–5.16 wt%) although in lunar parlance they are all considered to be low-Ti basalts (Neal and Taylor, 1992). Olivine basalts are lowest in TiO_2 (2.86 to 3.00 wt%), pigeonite basalts are slightly higher (3.29 to 3.38 wt%), and ilmenite basalts are demonstrably elevated (4.78 to 5.16 wt%) (Table 1). These seven fine-grained basalts are also lower in Al_2O_3 (8.06–10.1 wt%) and K_2O (0.06–0.07 wt%) than are the Apollo 14 and Luna 24 basalts, but they overlap those from Apollos 11, 15, and 17 (Neal and Taylor, 1992).

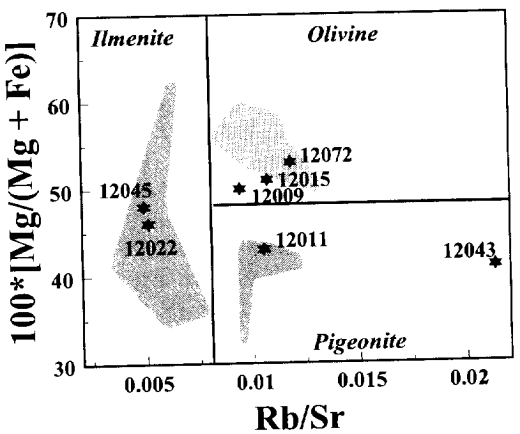

Fig. 1: Rb/Sr (weight ratio) vs. Mg for Apollo 12 basalts. Fields are shown for previously determined Apollo 12 mare basalt data; large stars = vitrophyres and fine-grained basalts analyzed in this study.

Our trace-element abundances of the seven samples—three olivine basalts (12009, 12015, and 12072), two pigeonite basalts (12011 and 12043), and two ilmenite basalts (12022 and 12045)—are presented in Table 1. A selection of these elements has also been plotted relative to C1 chondrites in Fig. 2. Relative HREE distributions are similar for all seven basalts. Olivine basalt 12072 has the lowest abundances of nearly all of the elements (except possibly Rb, La, and Ce, which may have been slightly affected by a higher relative proportion of mesostasis or addition of a KREEP-like component). The two other olivine basalts, 12009 and 12015, have higher REE abundances, within the range for pigeonite basalts, albeit lower than ilmenite basalts (Fig. 2a-c). Two of the samples, pigeonite-basalt 12011 and olivine-basalt 12072, exhibit roughly flat LREE (La/Nd(n) = 1.06–1.10; Fig. 2a,b), whereas the other five samples are distinctly LREE depleted (La/Nd(n) = 0.656–0.857). The most LREE-depleted sample, ilmenite basalt 12022 (Fig. 2c), contains the most REEs, Y, Zr, Cu, Ga, Th, Sr, and Hf. As pointed out in Neal et al. (1994b), these various basalt groups cannot be related to each other by simple fractional crystallization of observed liquidus phases.

Other trace-element relationships are also diagnostic of the specific basalt groups. Olivine basalts have the lowest light lithophile element (Li, Be) abundances (6.0–7.6 ppm and 0.18–0.61 ppm, respectively), and there is significant overlap in the Li and Be abundances in the ilmenite and pigeonite basalts (8.5–11 ppm and 0.43–0.81 ppm, respectively; Table 1). As pointed out by Rhodes et al. (1977), olivine basalts also contain the highest abundances of the compatible element Ni (55.0–73.5 ppm) and overlap in Cr concentration with ilmenite basalts (2470–3960 ppm). The ilmenite basalts are depleted in Ba and Nb relative to the pigeonite basalts, which have the highest Ba contents of all Apollo 12 basalts. Rubidium, Sr, and Sc abundances show the most systematic differences between basalt groups. Olivine basalts have the lowest Sr and Sc and intermediate Rb abundances, pigeonite basalts have higher Sr and Sc and the highest Rb abundances, and ilmenite basalts have the highest Sr and Sc and lowest Rb abundances. It is because of this systematic difference in Rb and Sr that Neal et al. (1994b) utilized the Rb/Sr ratio in concert with Mg to classify the Apollo 12 basalts (Fig.1).

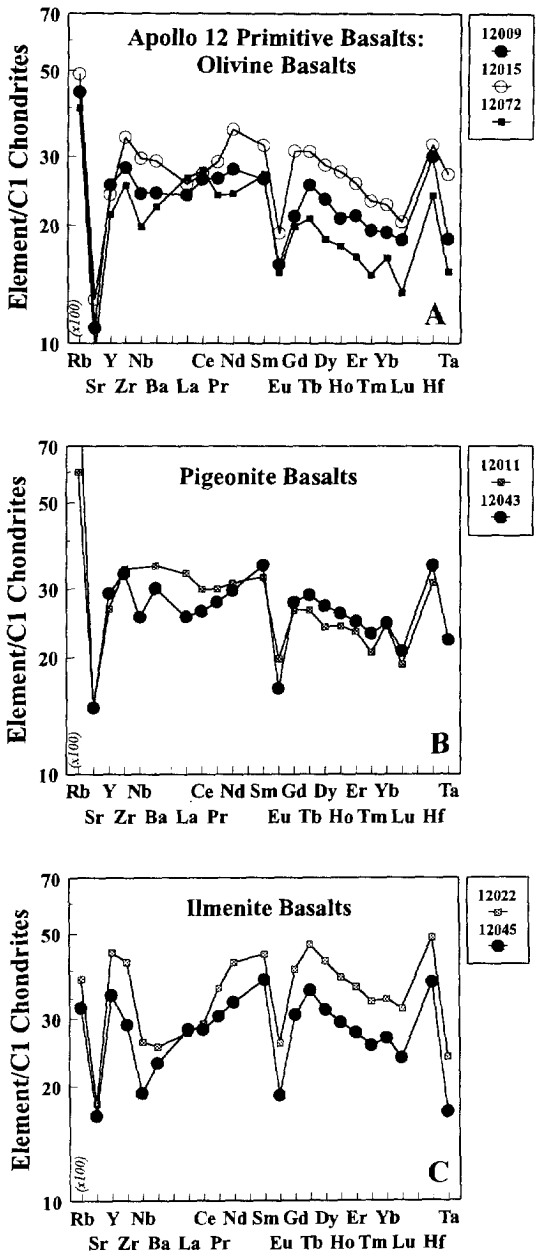

Fig. 2: Selected trace-elements in Apollo 12 vitrophyres and fine-grained basalts normalized to C1 chondrites (Wasson and Kallemeyn, 1988): (A) olivine basalts, (B) pigeonite basalts, (C) ilmenite basalts.

6. ISOTOPIC CHEMISTRY

6.1. Ages

Three fine-grained, parental, low-Ti basalts collected at the Apollo 12 landing site have been analyzed previously for their Ar-Ar isotopic compositions (Stettler et al., 1973; Alexander and Davis, 1974). These include two ilmenite basalts which yielded ages of 3.18 ± 0.07 and 3.20 ± 0.04 Ga (two splits of 12008) and 3.11 ± 0.04 Ga (12022). Two splits of an olivine basalt, 12009, also were analyzed and gave ages of 3.17 ± 0.07 and 3.29 ± 0.07 Ga. These analyses allow for a relatively broad range in ages from 3.07 to 3.36 Ga. However, as we will show below, it is much more likely that the vast majority of low-Ti basalts collected from the Apollo 12 landing site were extruded over a relatively narrow time interval, possibly within 20–50 million years.

Geochronologic information has been elicited from numerous other coarser-grained, low-Ti basalts from the Apollo 12 landing site. These include Rb-Sr and Ar-Ar studies by various groups of seventeen additional samples (Papanastassiou and Wasserburg, 1970; Compston et al., 1971; Murthy et al., 1971; Papanastassiou and Wasserburg, 1971a; Papanastassiou and Wasserburg, 1971b; Turner, 1971; Stettler et al., 1973; Alexander and Davis, 1974; Horn et al., 1975; Nyquist et al., 1977; Nyquist et al., 1979; Nyquist et al., 1981) and Sm-Nd studies of three of the same rocks (Nyquist et al., 1977; Nyquist et al., 1979; Nyquist et al., 1981). Previous studies have shown that, within their respective groups, these basalts are similar in mineralogy, mineral-chemistry, and whole-rock chemistry and are probably cogenetic (Dungan and Brown, 1977; Rhodes et al., 1977; Neal et al., 1994b). If individual basalt samples within a given group can be related by magmatic processes, then these basalts should be coeval. Thus, weighted-average ages have been calculated for the various mare basalt groups collected from the Oceanus Procellarum. The weighted-average ages of the three main mare basalt groups are quite similar: 3.19 Ga for olivine basalts, 3.18 Ga for pigeonite basalts, and 3.20 for ilmenite basalts. The one anomalous sample from the "feldspathic" group, 12038, appears to have an older crystallization age of 3.28 Ga.

6.2. Rb-Sr and Sm-Nd Abundances and Isotopic Compositions

During the present study, Rb, Sr, Sm, and Nd abundances and Nd and Sr isotopic compositions have been measured on splits of five of the fine-grained basalts/vitrophyres from the Apollo 12 landing site: two olivine basalts, 12009 and 12015, one pigeonite basalt, 12011, and two ilmenite basalts, 12022 and 12045 (Table 2). Ilmenite-basalt vitrophyre 12008 was analyzed for both Sm-Nd and Rb-Sr isotopic compositions and elemental abundances by Nyquist et al. (1979). Their data will be included in our discussions. As with previous workers, and by way of confirmation of the relative abundances determined by ICP-MS, the ilmenite basalts have the lowest Rb abundances, and the pigeonite and olivine basalts are similar and higher in Rb. Strontium abundances determined by isotope dilution also generally agree well with those determined by ICP-MS. Sm and Nd abundances do not differ between the two methods by more than 10% relative, and the Sm/Nd ratios of the three groups are confirmed by isotope dilution measurements.

These fine-grained Apollo 12 basalts are plotted in Fig. 3 (as time, in Ga, vs. ϵ_{Nd}), along with previous results from other Apollo 12 basalts (and fields for Apollo 11, 15, and 17 basalts). Apollo 12 basalts are among the youngest in the Apollo collections and span the greatest range in ϵ_{Nd}.

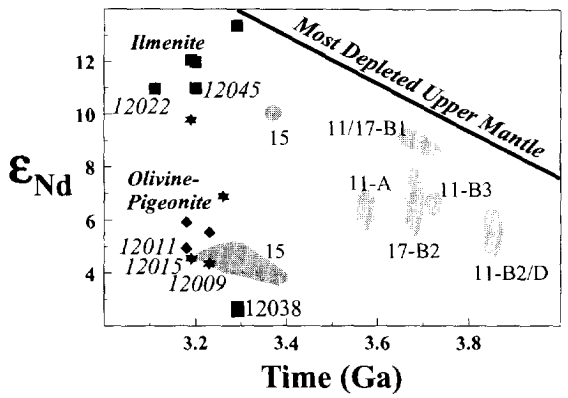

Fig. 3: ϵ_{Nd} of Apollo 12 basalts relative to crystallization age (in Ga). Olivine basalts are indicated by patterned stars, pigeonite basalts by dark diamonds, and ilmenite basalts by patterned squares. Sample numbers are indicated for the "new" fine-grained basalts and vitrophyres. Also shown are fields for other low-Ti (Apollo 15) and high-Ti (Apollo 11 and 17) mare basalts.

Two distinct populations are apparent among the Apollo 12 basalts—the combined olivine- and pigeonite-basalt supergroup and the ilmenite-basalt supergroup. Olivine basalts 12009 and 12015 yield similar initial Sr ($^{87}Sr/^{86}Sr$ = 0.69954–0.69960) and Nd (ϵ_{Nd} = +4.3– +4.5) isotopic ratios (Table 2). Pigeonite basalt 12011 was analyzed for Nd isotopes by Unruh et al. (1984) and yielded an ϵ_{Nd} value at 3.2 Ga of +4.1 ± 0.6, well within analytical uncertainty of our split. Pigeonite and olivine basalts yield similar T_{LUM} model ages (LUM = Lunar Upper Mantle as per Snyder et al., 1994; see section 3.) of 4.12–4.15 Ga. Ilmenite basalts are distinctly different in Nd isotopic composition, having ϵ_{Nd} values (at 3.2 Ga) of +10.5 ± 0.6 to +11.2 ± 0.5 and T_{LUM} = 3.82–3.87 Ga. Furthermore, the $^{147}Sm/^{144}Nd$ ratios of the two supergroups (olivine-pigeonite and ilmenite) are also significantly different (Table 2) and require two distinct sources.

Within analytical uncertainty, the initial Sr isotopic compositions of the pigeonite and olivine basalts are the same, thus suggesting an isotopically similar source. On the other hand, the initial Sr isotopic compositions of the ilmenite basalts are quite different and are consistent with a mantle source region formed just after accretion of the Moon (T_{LUNI} = 4.56 to 4.59 Ga; Table 2, Fig. 4). The single pigeonite basalt gives a similar model age of 4.48 Ga, but the olivine basalts yield slightly lower, although statistically similar, model ages of 4.31– 4.44 Ga.

7. THE LUNAR MAGMA OCEAN AND CUMULATE SOURCE FORMATION

Various workers (Shih and Schonfeld, 1976; Hughes et al., 1988, 1989; Snyder et al., 1992; Snyder and Taylor, 1993; Shearer and Papike, 1993) have presented varied, yet extensive, models of the crystallization of an incipient lunar magma ocean (LMO) that include the major- and trace-element and mineralogic composition of the consequent cumulates. A fundamental tenet of all of these models is that, once plagioclase becomes a liquidus phase, it is efficiently separated from associated mafic cumulates by flotation to form the lunar crust. These mafic cumulate regions compose the lunar upper mantle and are likely to be the sources for most mare basalts collected from the Moon. Whereas our group (e.g., Snyder et al., 1992, and references therein) and many others (e.g., Hess and Parmentier, 1995, and references therein) have studied the dynamic, chemical, and mineralogic evolution of high-Ti basalt source regions in great detail, the source regions of low-Ti basalts, which are likely to compose over 95% of the upper mantle, have been largely ignored of late.

A first-order observation of all mare basalts is that, compared to their terrestrial counterparts, the most primitive samples have Mg#s [$Mg^{2+}/(Mg^{2+}+Fe^{2+})$] that indicate significant evolution from a chondritic composition. This evolution either occurred en route to the surface or is representative of the mantle source region. Most workers have concluded that most of this evolution is inherited from the source region (Nyquist and Shih, 1992, and references therein; Snyder et al., 1992; Snyder and Taylor, 1993).

A major consequence of the hypothesized lunar magma ocean differentiation model (e.g., Warren, 1985) is that the Moon's upper mantle should be quite evolved in terms of Mg #. The upper mantle may have been initially layered due to crystallization in a deep LMO, analogous to that which is observed in layered mafic intrusions on Earth. The relatively low viscosities of lunar magmas (10 to 100 poise; Taylor and Lu, 1992) allows the LMO to have undergone vigorous convection (Ra = 10^{23} to 10^{25}; Snyder and Taylor, 1992). Such vigorous convection likely would have continued during early crystallization of the LMO. Thus, equilibrium crystallization would have prevailed in the LMO until it became just above 50% crystalline, at which point convection would have begun to slow and cease (Marsh and Maxey, 1985), and fractional crystallization would have taken place (Snyder et al., 1992).

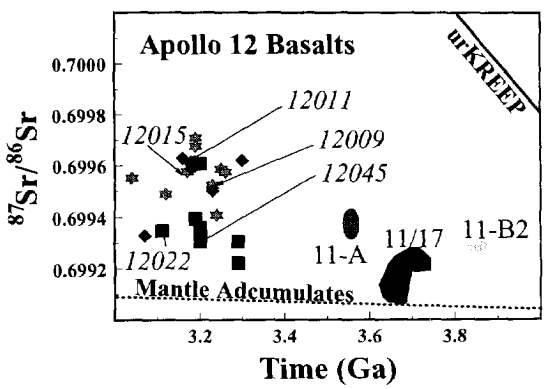

Fig. 4: Initial $^{87}Sr/^{86}Sr$ relative to crystallization age (in Ga) for all Apollo 12 basalts. Olivine basalts are indicated by patterned stars, pigeonite basalts by dark diamonds, and ilmenite basalts by patterned squares. Sample numbers are indicated for the "new" fine-grained basalts and vitrophyres. Also shown are evolution lines for lunar upper mantle ("mantle adcumulates") and residual magma ocean liquid ("urKREEP"). Fields for the Apollo 11 Groups A and B2 and Apollo 11 B1-B3 + Apollo 17 high-Ti basalts are also indicated.

7.1. Major-Element Evolution

The prolonged period of equilibrium crystallization serves to buffer the differentiation of the LMO and, thus, the Mg. In fact, during the first 75% of LMO evolution, when equilibrium crystallization is likely predominant, the Mg # of the LMO and, thus, the crystallization products of the LMO, changes less than 10%, from 93 to 85 (Snyder and Taylor, 1993). Based on known Fe-Mg partitioning in minerals and likely scenarios for melting of the upper mantle cumulate, this means that magmas generated from the lower 75% of the lunar upper mantle are too primitive to be considered the source for any group of mare basalts, although they could be parental to picritic glasses (Longhi, 1987). Only sources formed after about 75–80% crystallization of the LMO, and originally very shallow, can be considered the sources for the lunar mare basalts. This is supported by the well-established observation that mare basalts exhibit rather large negative Eu anomalies consistent with prior removal of plagioclase, and plagioclase becomes a liquidus phase in most LMO differentiation models after 60–80% crystallization (e.g., Snyder and Taylor, 1993).

Assuming that the most primitive of the fine-grained and vitrophyric Apollo 12 basalts have not undergone extensive differentiation either en route to the surface or at the surface, we can estimate that their source regions had Mg #s of ~70 for the olivine basalts, ~65 for the ilmenite basalts, and ~60 for the pigeonite basalts. These Mg #s correspond to sources formed after 87–89% crystallization of the LMO, and these levels would fall within the range of cumulates that would be dominated by subequal proportions of clinopyroxene, plagioclase, and pigeonite. However, Neal et al (1994b) have indicated that olivine is required in the sources for the Apollo 12 basalts. Thus, a mechanism is needed to bring olivine-bearing cumulates from below or to bring more fertile source regions down to the olivine-bearing cumulates.

Several workers have indicated that the crystallization products of an LMO would be inherently unstable with more-dense, Fe-rich cumulates lying above less-dense, Mg-rich cumulates (Ringwood and Kesson, 1976; Ryder, 1991; Hess and Parmentier, 1993). These authors have suggested that the lunar mantle, after complete solidification, would undergo catastrophic overturn. Hess and Parmentier (1993) even suggested that late-crystallizing ilmenites could sink through the LMO cumulate pile to form the lunar core. However, Snyder and Taylor (1993) have indicated some of the pitfalls in this model. Instead, we have supported more localized, subsolidus overturn during precipitation of the lunar upper mantle (Snyder et al., 1992), which would serve to mix shallow, olivine-free sources with deeper, olivine-bearing sources. In subsequent melting models, we will assume an olivine-bearing residue, in accord with the work of Neal et al. (1994b).

7.2. Trace-Element Evolution

Hughes et al. (1988, 1989), Snyder et al. (1992), and Snyder and Taylor (1993) presented models for evolution of the LMO with an initial starting composition for most lithophile trace elements that was ~3x chondritic. The rationale for this choice of values is that the LMO was likely a melt of ~30% of the total Moon that was roughly chondritic in most refractory, lithophile-element abundances. This proportion of melting of the whole Moon leads to an LMO cumulate upper-mantle that is ~500 km deep and is supported by seismic data (Nakamura, 1983; Mueller et al., 1988; Kuskov, 1995). The deep lunar interior is probably composed mostly of olivine and orthopyroxene in which large-ion, lithophile elements are incompatible; therefore, these elements are effectively enriched in the LMO by a factor of ~3.

The original estimate of the initial LMO abundances of Rb and Sr were 1.0 and 34.2 ppm, respectively (Snyder et al., 1992), yielding a Rb/Sr weight ratio of 0.029. In a subsequent study, this was adjusted to ~0.35 ppm Rb and 11 ppm Sr (Snyder and Taylor, 1993), based on multiplying the primitive bulk Moon Rb abundance (0.12 ppm) of O'Neill (1991) by a factor of 3 to attain the initial LMO composition. This bulk Moon abundance is predicated on the hypothesis that nearly all of the volatile element budget of the Moon was added as a late veneer of infalling chondritic material (O'Neill, 1991). However, the Rb/Sr ratio of the bulk Moon is probably much lower than 0.029, as most estimates vary from 0.006 to 0.009, with an average of 0.007 (Taylor, 1982; O'Neill, 1991; McDonough et al., 1992). Therefore, assuming that our Rb abundance for the LMO is 0.35 ppm and the Rb/Sr weight ratio of the initial LMO is similar to the bulk Moon (0.007), the Sr abundance of the initial LMO is estimated at 50 ppm.

Whereas the LMO cumulate sources for most mare basalts are likely located in the upper 25% of the upper mantle, we have modelled the composition of these sources by combining olivine-pigeonite-clinopyroxene adcumulates with varied proportions of trapped residual LMO liquid. The high-Ti mare basalts indicate 0.8–1.5% trapped liquid in the source (Snyder et al., 1994). In contrast, the source of the ilmenite basalts had less than 0.2% trapped liquid in the cumulates and the olivine and pigeonite basalts were derived from a similar source with 0.4 to 0.5% trapped residual liquid (Fig. 5).

We have also included the light-lithophile elements Li and Be in our LMO modelling and have used the Li and Be abundances (0.83 and 0.18 ppm, respectively) for the bulk silicate Moon from Taylor (1982). The value for Li is somewhat lower than that proposed by O'Neill (1991) (1.9 ppm Li). The proposed Li/Be ratio (4.6; Taylor, 1982) is similar to that determined from mare basalts (3–5; Dreibus et al., 1976), but much lower than that suggested from picritic glasses (10–34; Shearer et al., 1994). We have evaluated the LMO modelling using both sets of Li, Be, and Li/Be data. If the latter set of higher Li, Be, and Li/Be is used for LMO modelling, calculated residual LMO liquids are even higher than those values measured for the low-Ti basalts and picritic glasses. Thus, the degree of melting of LMO-derived cumulate sources that would be needed to yield low-Ti mare basalts would be undefined. Therefore, either the LMO crystallization models previously presented are seriously in error, or the initial silicate Moon had values similar to those pro-

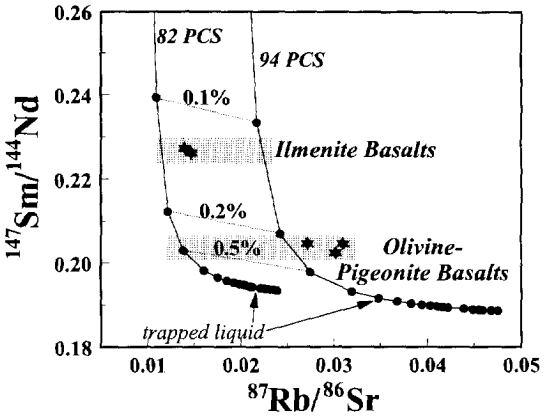

Fig. 5: $^{147}Sm/^{144}Nd$ relative to $^{87}Rb/^{86}Sr$ for the Apollo 12 fine-grained and parental basalts. Also indicated are mixing arrays for upper mantle LMO adcumulates at 82 PCS (per cent solid) and 94 PCS (per cent solid) with trapped residual liquid. Percentages on this plot are the proportions of trapped liquid in the upper mantle cumulates.

posed by Taylor (1982) and Dreibus et al. (1976). We have elected to follow the latter alternative. In order to calculate the initial LMO composition, we again assumed that the bulk Moon was ~30% partially melted, leaving an olivine-orthopyroxene residue. Thus, the initial LMO composition is 1.80 ppm Li and 0.52 ppm Be (mineral/melt partition coefficients for olivine and orthopyroxene from Shearer et al., 1994).

8. PARTIAL MELTING OF THE LOW-Ti MANTLE SOURCES

In order to model the formation of mare basalt magmas, we have taken calculated cumulates at various stages of crystallization of the LMO and calculated the effects of varying degrees (typically 1–10%) of partial melting. We use the batch modal melting equation,

$$C_L = C_o / [D_o + F(1-D_o)] \quad (4)$$

where C_L = concentration of an element in the derivative melt, C_o = concentration of the element in the initial cumulate solid, D_o = bulk minerals/melt distribution coefficient, and F = fraction of melt. Mineral/melt partition coefficients are compiled in Snyder and Taylor (1993) and Shearer et al. (1994; for Li and Be).

We have also evaluated the effect of trapped, residual LMO liquid in the cumulate sources for low-Ti mare basalts. As a first approximation and an endmember of possibilities, we have assumed that this trapped residual liquid makes up 1% of the total cumulate and is always the first "phase" to melt. Thus, a 1% partial melt would be composed of only this trapped liquid component, a 2% partial melt would contain one-half trapped liquid, a 5% melt would be one-fifth trapped liquid, etc.

Based on a host of trace-element data, Neal et al (1994b) have determined quantitative models for the sources of Apollo 12 low-Ti basalts. In particular, they found a plot of Co/Hf relative to Sc/Sm (Fig. 6) as the most diagnostic of varied mantle melting, as well as post-extrusive differentiation. The subparallel lines on Fig. 6 represent primitive melts of the mantle source. The lower line represents the composition of partial melts of the ilmenite-basalt source composed of 45.5% olivine + 42.5% pigeonite + 11.5% clinopyroxene + 0.5% plagioclase. The upper line represents the composition of partial melts of the pigeonite-olivine-basalt source composed of 48% olivine + 22% pigeonite + 30% clinopyroxene. Those basalts lying above their respective lines have accumulated minerals after extrusion and those lying below the lines have lost minerals and represent residual liquids after fractionation.

8.1. Source Constraints from Experimental Petrology

If one can rule out polybaric fractional fusion in a mantle diapir as a likely mechanism (Longhi, 1992a), liquidus mul-

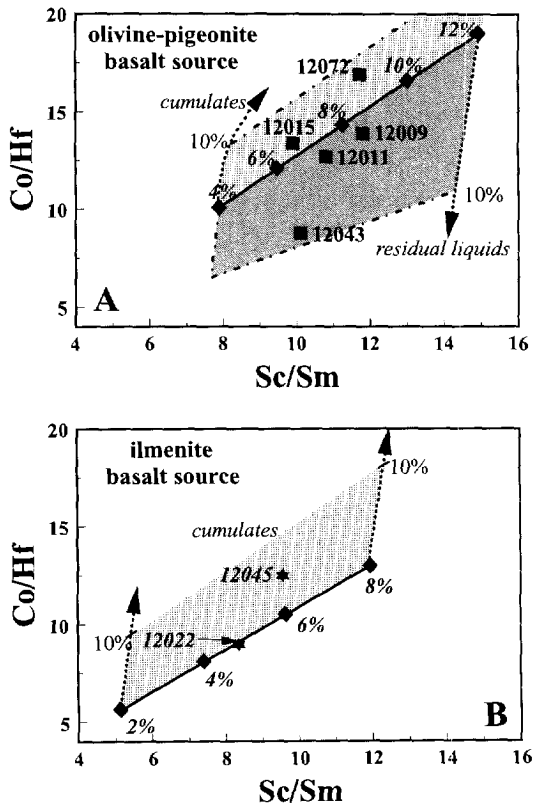

Fig. 6: Plots of ratios of moderately compatible elements, Co/Hf, vs. compatible/incompatible element ratios, Sc/Sm, for fine-grained ilmenite, olivine, and pigeonite basalts. The diagonal dark lines on both plots include primary magmas generated by varied degrees of partial melting of a low-Ti upper mantle source as described in the text (and from Neal et al., 1994b). Diamonds = 2% melting intervals for their respective sources. (A) For the olivine-pigeonite-basalt source. The field above the source encompasses all plausible cumulates with up to 10% accumulated minerals. The field below the source encompasses the complementary residual liquids from accumulation of 10% minerals (as per Neal et al., 1994b). (B) for the ilmenite-basalt source with fields similar to (A).

tiple-saturation experiments yield important information about the depth of melting and the composition of the source regions for mare basalts (Longhi, 1992b). Polybaric fractional fusion is often difficult to assess in a group of presumably related basalts; however, if it can be proven that this process did operate, multiple-saturation experiments should yield a weighted-average pressure of melting.

Liquidus multiple-saturation experiments have been performed on six natural low-Ti basalts from the Apollo 12 collection (Walker et al., 1976; Green et al., 1971a; Green et al., 1971b) and one synthetic basalt (Kushiro et al., 1971). These studies included samples from all three main groups: olivine basalts 12002, 12009, and 12040; pigeonite basalts 12021 and 12065; and ilmenite basalt 12022. If these results are evaluated (Longhi, 1992b) and only the most primitive parental basalts are utilized (ruling out samples that obviously have accumulated phases), the following general conclusions can be made. The sources for the low-Ti basalts from the Apollo 12 landing site contain predominantly olivine and low-Ca pyroxene (either orthopyroxene or pigeonite). Melting of the olivine-basalt source occurred at pressures from 5–13 kb, corresponding to depths of 100–250 km in the Moon (Warren, 1985). Ilmenite basalts seem to be derived from a much deeper source (14–15 kb; 300–400 km). The depths of melting for pigeonite basalts are not well-defined because primitive compositions from this group have not been studied. However, if the sources for the olivine and pigeonite basalts are similar, if not the same (see below), these two groups of basalts could have been derived from similar depths (100–250 km).

8.2. Ilmenite-Basalt Source

The much higher initial $^{143}Nd/^{144}Nd$ ratios for the ilmenite basalts relative to the pigeonite and olivine basalts is definitive evidence of a different source (Fig. 3). The chemical compositions of fine-grained ilmenite basalts 12022 and 12045 are consistent with their derivation by 5% and 6% nonmodal partial melting, respectively (Fig. 6a). This degree of partial melting of the ilmenite-basalt source is the same as that suggested by Nyquist et al. (1979). Basalt 12022 lies on the ilmenite-basalt source melting line, thus indicating a primitive, undifferentiated melt. However, basalt 12045 lies just above the ilmenite-basalt source melting line. This sample has a higher proportion of plagioclase and mesostasis and a much lower proportion of olivine than 12022, possibly indicating some crystal accumulation and fractionation after extrusion and suggesting that it is not a truly primitive, parental composition. The behavior of 12045 is in contrast to that of most other ilmenite basalts, which plot below the source melting line, indicating that they have precipitated up to 10% of their weight in crystals leaving a more evolved residual liquid.

8.3. Pigeonite and Olivine Basalt Source

The initial $^{143}Nd/^{144}Nd$ ratios are the same for the olivine and pigeonite basalts (Fig.3), consistent with a similar source for both basalt groups. The main difference in the two basalt groups is the evidence for crustal assimilation, in terms of Al_2O_3-Co covariation and decreasing Sm/Eu and Rb/Sr with differentiation in the pigeonite basalts (Neal et al., 1994b). Whereas the olivine basalts have been modelled by up to 25% crystal accumulation (presumably at the surface) in magmas that were generated by 5–11% partial melting of the source, modeling of pigeonite basalts involved significant assimilation-fractional crystallization with a crustal component (Neal et al., 1994b). However, there is no evidence from isotopic studies (see above) that contamination has affected the fine-grained, pigeonite basalts presented within.

Fine-grained basalt data indicate variable degrees (12009 = ~9%; 12011 = ~7%; 12015 = ~7%; 12043 = ~7%; 12072 = ~8%) of nonmodal equilibrium melting of the source (Fig. 6b). Olivine basalt 12072 has undergone a small degree (<10%) of fractional crystallization after extrusion, due to precipitation of olivine and accumulation of pyroxene and plagioclase (Fig. 6b). Pigeonite basalt 12043 also indicates precipitation of a small amount of olivine (<10%), leaving a residual liquid depleted in this component (Fig. 6b). The overall primitive nature of the the two fine-grained pigeonite basalts (especially 12011) and the similarity of their isotopic compositions suggest that, if assimilation-fractional crystallization was significant in their genesis, it must have occurred prior to extrusion and to similar degrees in both 12011 and 12043. Thus, these two pigeonite basalts probably were derived from the same magma batch. Conversely, these two fine-grained pigeonite basalts may be indicating that assimilation was not an important process in their genesis. That the olivine basalts, which do not show evidence of crustal assimilation, have similar isotopic compositions to the fine-grained pieonite basalts points to this latter alternative.

8.4. Light Lithophile Element (Li, Be) Systematics of Low-Ti Sources

The light lithophile elements (Li, Be, and B) are an important class of elements for the study and modelling of magmatic processes on the Moon. Norman and Taylor (1992) presented evidence that the Li-REE systematics of mare basalts and highlands crustal rocks "track the evolution of the Moon's crust and mantle during crystallization of the magma ocean." Therefore, the Li-Be systematics of Apollo 12 basalts may be crucial in further elucidating their mantle sources. Li behaves as a moderately incompatible, and B and Be as highly incompatible, elements in mafic systems (Ryan and Langmuir, 1987, 1988, 1993). On Earth, the determination of igneous processes from Li and B abundances is compromised by their solubility in hydrothermal fluids. However, the anhydrous nature of the Moon removes this complication, allowing use of the light lithophile elements as tracers of magmatic processes (e.g., Shearer et al., 1994).

The Li-Be systematics of the seven fine-grained basalts (Table 1) are typical of those determined for other basalts at the Apollo 12 landing site (Cuttitta et al., 1971; Schnetzler and Philpotts, 1971; Wänke et al., 1971). Olivine basalts

typically have the lowest Li (4.5–7.5 ppm) and Be (~0.9 ppm) abundances, whereas pigeonite and ilmenite basalts overlap at higher abundances (6.1–8.4 ppm and 1.1–1.9 ppm, respectively). Beryllium abundances of the fine-grained basalts analyzed in this study are much lower than those of Apollo 12 basalts analyzed previously. This is likely due to the lower detection limit of the method used in our study and does not reflect true differences. Beryllium abundances of the fine-grained olivine basalts were found to be lower than those in the pigeonite and ilmenite basalts, consistent with previous analyses.

The Li/Yb ratios of previously analyzed Apollo 12 low-Ti basalts are unique with similar values of ~2 at Li abundances from 6.7 to 10.8 (Schnetzler and Philpotts, 1971). The seven fine-grained basalts analyzed in this study also fall within this tight range (Fig. 7), whereas low-Ti basalts from Apollo 15 generally have higher Li/Yb ratios (~3). High-Ti mare basalts from the Apollo 11 and 17 sites have Li/Yb ratios of ~1. Picritic glasses from all landing sites, excluding Apollo 12, have Li/Yb ratios in excess of 3. Highlands rocks, which are generally enriched in plagioclase with a high Li/Yb ratio, also have Li/Yb values in excess of 3 (and up to 100), along with Li abundances of <8 ppm (Norman and Taylor, 1992). Li/Yb ratios of KREEP are ~1, but with Li abundances in excess of 20 ppm (Fig.7a).

Li-REE systematics of Apollo 12 fine-grained basalts suggest that they are derived by partial melting of cumulate sources after 84%–94% crystallization of the LMO (Fig. 7a). This is consistent with that determined solely on Fe-Mg characteristics of the basalts and potential sources (after 87–89% crystallization of the LMO; see above). However, only very small percentages of partial melting (generally <0.5%) of an *adcumulate* source will generate the Apollo 12, low-Ti basalts (Fig. 7a). Instead, if a small proportion of trapped, residual-LMO liquid (~1%) is assumed in the initial source, as is suggested by LMO modelling (Hughes et al., 1988, 1989; Snyder et al., 1992) and Nd-Sr isotopic and abundance studies (Snyder et al., 1994; also see Fig. 5), more realistic proportions of melting are suggested (Fig. 7b). In fact, the Apollo 12 basalts indicate from 1.5% (12022) to 5% (12043) partial melting of upper mantle cumulate sources. If smaller proportions of trapped liquid are assumed in the initial cumulate source, smaller degrees of partial melting would be needed to generate the low-Ti mare basalts. In any event, partial melting of upper-mantle, cumulate sources, formed after 84%–94% crystallization of the LMO and containing a small proportion of trapped, residual liquid, will generate parental magmas that can fractionate to give all low-Ti mare basalts. Residual LMO liquids, after ~ 98% crystallization, yield Li-Be-Yb compositions similar to postulated urKREEP (Fig. 7a), consistent with other elemental LMO modelling (e.g., Snyder and Taylor, 1993).

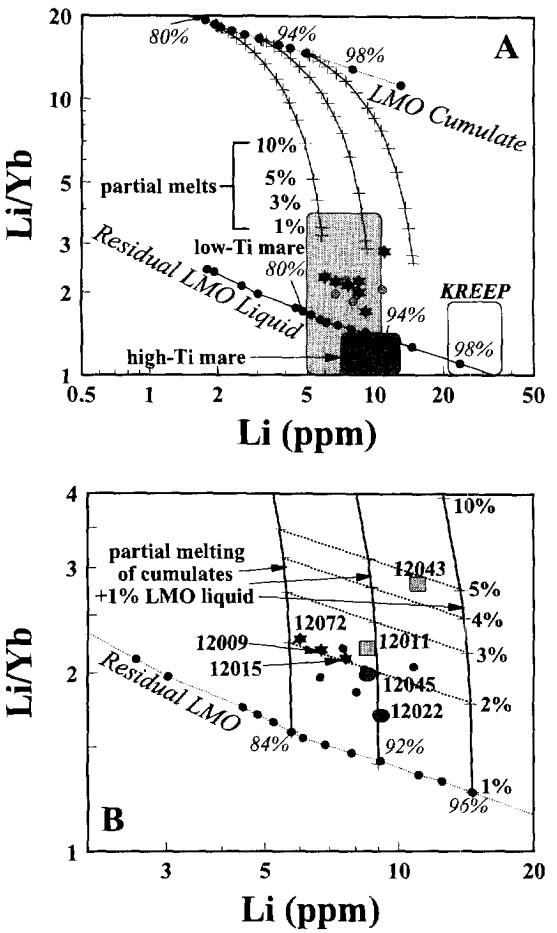

Fig. 7: Li (ppm) relative to Li/Yb for fine-grained Apollo 12 mare basalts. (A) Apollo 12 fine-grained basalts relative to other low-Ti and high-Ti mare basalts (Schnetzler and Philpotts, 1971). Also shown are evolutionary arrays for LMO residual liquids and adcumulates and curves indicating degrees of partial melting of upper mantle LMO cumulates (generated after 84, 92, and 96% crystallization of the LMO). Stars = fine-grained and vitrophyric Apollo 12 parental basalts; lightly shaded circles = other Apollo 12 basalts (Schnetzler and Philpotts, 1971). (B) An expansion of a portion of figure (A) and taking into account 1% trapped residual LMO liquid in the cumulate source (e.g., Snyder et al., 1992). Lower dashed diagonal line shows the evolution of the residual LMO liquid (the LMO cumulate would plot above the diagram). Nearly vertical lines represent progressive degrees of partial melting of LMO-derived cumulates after 84, 92, and 96% crystallization. Numbers to the right of the 96% crystallized LMO cumulate lines are percentages of partial melting. Dashed diagonal lines are for similar proportions of partial melting. Key: stars = olivine basalts; squares = pigeonite basalts; ovals = ilmenite basalts.

9. DISCUSSION

Snyder et al. (1994) speculated that the source for the ilmenite basalts at Apollo 12 may have been the same, or a similar source, to that which yielded the older high-Ti volcanics at the Apollo 11 and 17 landing sites. Thus, the mantle source for these rocks would have to be widespread within the lunar interior and would have had to persist from 3.85 Ga (earliest high-Ti volcanism; Groups B2 and D basalts; Snyder et al., 1996) to 3.2 Ga, a period of nearly 700 million years. Snyder et al. (1994) postulated that the source of the high-Ti basalts was depleted in ilmenite and trapped liquid by continued melting, yielding a source that was less Ti enriched and more LREE depleted. Thus, magmas generated

at 3.2 Ga would reflect this changing source, yielding the characteristic high ϵ_{Nd} ilmenite basalts. However, recent Lu-Hf isotopic studies tend to refute this argument. Beard et al. (1994; 1996) point out that the ilmenite basalts are similar in their Lu-Hf isotopic compositions to all other low-Ti basalts, including Apollo 12 and 15 basalts, and differ markedly from the high-Ti mare basalts.

We have assumed in our isotopic studies of high-Ti basalts (Snyder et al., 1994; Snyder et al., 1996) that their Sm/Nd ratios are similar to their source regions. However, Nyquist et al. (1977; 1979) have shown that, whereas this is roughly true for high-Ti mare basalts, it is far from truth for low-Ti mare basalts from the Apollo 12 landing site. In fact, they suggest that the $^{147}Sm/^{144}Nd$ ratios of the ilmenite and olivine-pigeonite basalts may have decreased by 13%–18%, respectively, as a consequence of small degrees of partial melting and smaller proportions of high-LREE phases in the residue (i.e., clinopyroxene and plagioclase). Thus, the relatively low T_{LUM} model ages (4.13–4.15 Ga for olivine-pigeonite basalts and 3.82–3.87 Ga for ilmenite basalts) for the low-Ti basalts are evidence of Sm/Nd fractionation during melting, with ilmenite basalts showing greater fractionation than olivine-pigeonite basalts, consistent with the calculations of Nyquist et al. (1979). Anomalies in the abundances of the short-lived radionuclide ^{142}Nd for several low-Ti mare basalts is convincing evidence that their source regions were created early in lunar evolution, reached isotopic closure at ~4.32 Ga, and were not significantly modified until melting to form the basalts (Nyquist et al., 1995).

The upper mantle source for the ilmenite basalts was likely formed earlier in the crystallization of the LMO, prior to formation of the source for the high-Ti basalts, and ilmenite is not required in the residue for the ilmenite basalts (Neal et al., 1994b; Shearer et al., 1996). This might suggest that the ilmenite-bearing source only existed in the region beneath Mare Serenitatis and Mare Tranquillitatis, in the eastern near-side. However, analyses of picritic glasses from all landing sites (Delano, 1986) have shown the proclivity for these samples to be high-Ti in tenor. Even picritic glasses retreived from notably low-Ti mare sites, such as Apollo 12 and Apollo 15, have high-Ti abundances. Furthermore, Apollo remote-sensing data, in concert with telescopic observations of the volcanic stratigraphy in Oceanus Procellarum, show clearly that the oldest units (Repsold Formation) contain high-Ti flows that are possibly correlative with those in Mare Serenitatis and Mare Tranquillitatis. Thus, it is likely that high-Ti basalt volcanism was one of the earliest, widespread, volcanic events on the lunar near-side.

There is abundant evidence that the mare basalts from a given landing site are notably dissimilar in their trace-element signatures to picritic magmas, represented by glass beads, from the same site (Longhi, 1987). The Li and Be abundances in fine-grained, low-Ti basalts (6.0–11 ppm, and 0.18–0.81 ppm, respectively) from Apollo 12 are vastly different from the abundances in the high-Ti (15.8–16.7 wt% TiO_2) "red" volcanic glasses (19.2 ppm Li and 1.14 ppm Be) from the same landing site (Shearer and Papike, 1993; Shearer et al., 1994). In fact, the Li and B abundances in this Apollo 12 red glass are the highest of any lunar picritic glasses yet analyzed (Shearer et al., 1994). It is likely that these elevated Li and Be abundances for Apollo 12 red glasses indicate derivation from volatile-undepleted lower mantle (e.g., Ringwood et al., 1992).

Mare basalts with elevated Ti contents are thought to be the consequence of melting of ilmenite-bearing layers formed late in the crystallization of the lunar magma ocean (Hughes et al., 1989; Snyder et al., 1992). The lower mantle of the Moon should be relatively primitive, composed of mostly olivine and orthopyroxene and extremely poor in ilmenite. If this is so, one would not expect picritic magmas, which come from the lower mantle, to have high Ti contents. How might primitive picritic magmas attain this high-Ti signature?

The high-Ti nature of many picritic magmas (extant as glass beads) must have been either inherited from the source region or introduced after initial melting in the source region. Spera (1992) stated that, due to density contrasts in lunar magma ocean cumulates, ilmenite-bearing layers from the uppermost portion of the upper mantle will sink relative to other cumulates in the upper mantle. This was first suggested as an important tenet of mare basalt genesis by Ringwood and Kesson (1976). However, Hess and Parmentier (1993) further project that most of the ilmenite will continue sinking until it forms a lunar core. They also consider it likely that some of this ilmenite will mix with the lunar mantle, thus creating fertile high-Ti source regions throughout the mantle. The mean depth of melting of high-Ti picritic magmas is estimated at 400–500 km near the base of the differentiated lunar upper mantle (Hess, 1993). However, the depth of incipient melting could be much greater than this, especially if one considers that picritic magmas were formed by polybaric fractional fusion (Longhi, 1992a). Therefore, high-Ti picritic magmas could be formed at a variety of depths throughout the lunar lower mantle.

10. A MODEL OF ANATEXIS OF THE LUNAR MANTLE

Combining telescopic observations and remote-sensing data with petrologic, elemental, and isotopic data from the Apollo collections, a clearer picture of the evolution and partial melting of the lunar interior is starting to emerge. Relatively rare "cryptomare" are probably the first evidence of melting of the lunar interior and subsequent extrusion of melts (Head and Wilson, 1992). However, we have no samples of this volcanic event in the Apollo collections and little idea on its character from telescopic observations. KREEP (K, REE, and P-enriched) basalts are among the oldest, pristine, volcanic rocks dated from the Apollo collections and vary in age from 3.8 to 4.1 Ga (Shih et al, 1992). However, these rocks are rare and there is, as yet, no evidence that they formed extensive flows or mare. So-called high-Al basalts are also among the oldest volcanic rocks in the Apollo collections; however, we have contended that these rocks are not true mare basalts but are probably impact melts of mixed derivation, the older ages reflecting the antiquity of the highlands component (Snyder and Taylor, 1996; Snyder et al., 1997). Therefore, Groups D and B2 high-Ti

basalts from the Apollo 11 landing site represent not only the earliest volcanic event (~3.85 Ga; Papanastassiou et al., 1977; Snyder et al., 1994; 1996) in the Apollo collections but among the earliest evidence of mare volcanism. That earliest mare volcanism was high-Ti in tenor is supported by telescopic observations (Whitford-Stark and Head, 1980; Head and Wilson, 1992).

10.1. Trapped Liquid and Depths of Melting

If KREEP basalts and Groups D and B2 high-Ti basalts are truly representative of early lunar volcanism (~3.85 Ga), then the earliest melts of the lunar interior were enriched in the incompatible elements. Some incompatible elements, namely K, U, and Th, have radioactive isotopes that are capable of producing the heat required for partial melting. Late-stage, residual liquids from crystallization of the LMO would also be enriched in incompatible elements such as the REE, K, U, and Th. It is considered likely that a small proportion (roughly <1–5%) of the residual, LMO liquid was trapped in upper mantle cumulates as they crystallized and is reflected in the changes in $^{147}Sm/^{144}Nd$ ratios of derivative, ilmenite-bearing, lunar basalts over time (Fig. 8). Enrichment of these incompatible elements in the residual LMO liquid would increase with crystallization; thus, late-forming LMO cumulates would trap liquid that is progressively more incompatible-element enriched. Furthermore, this residual LMO liquid would have been lighter than surrounding cumulates and would have likely migrated upward in the mantle over time. The uppermost portions of the lunar mantle should have had the highest proportion of trapped residual liquid

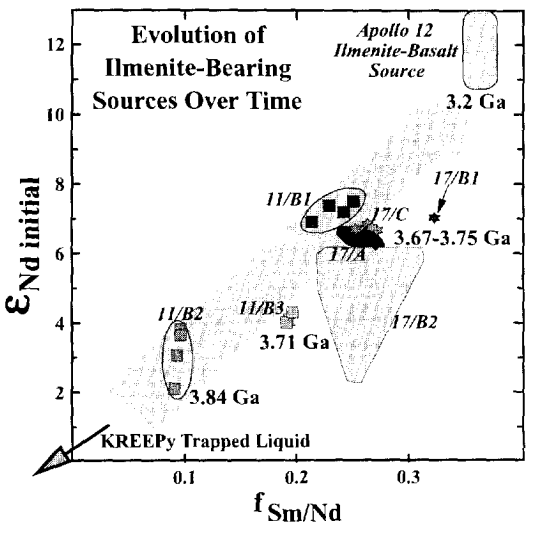

Fig. 8: Plot of $f_{Sm/Nd}$ (fractionation of Sm/Nd relative to chondritic Sm/Nd) vs. initial ϵ_{Nd} for all ilmenite-rich basalts from the Apollo collections (numbers indicate Apollo landing site and letters are the given basalt groups). Ages are also indicated (in Ga) adjacent to the basalt groups. The estimated source $^{147}Sm/^{144}Nd$ composition for Apollo 12 ilmenite basalts is taken from Nyquist et al. (1979). KREEPy, trapped, residual LMO liquid would project off the lower left of this diagram to negative ϵ_{Nd} and $f_{Sm/Nd}$ values. (After Snyder et al., 1994.)

with the most elevated incompatible-element abundances. LMO phase modelling also shows that the uppermost (>95% crystallization of the LMO) cumulate mantle should contain ilmenite. Thus, the most fertile site for partial melting is also the most Ti-enriched in the Moon. Radiogenic isotopic dating of Apollo 11 and Apollo 17 low-K, high-Ti mare volcanics indicates that this volcanic episode continued until about 3.67 Ga, i.e., for about 200 million years (Snyder et al., 1994).

The fertility of cumulate sources in the lunar upper mantle could have been controlled largely by the proportion of trapped residual liquid. The earliest volcanics, KREEP basalts, have proven difficult to interpret (e.g., Ryder, 1987; Shih et al., 1992). The KREEP basalts are probably melts of the deep lunar interior although the impetus for melting is difficult to ascertain (for one model, see Ryder, 1994). It may be that these melts are akin to the komatiitic plumes in the early Earth and may be formed by perturbations deep in the Moon. However, there is no doubt that these picritic basalts have somehow obtained a KREEP signature, possibly during transit to the surface through assimilation of KREEPy, residual, LMO liquid trapped in upper mantle cumulates. Those sources with 1.5–2% trapped, residual, LMO liquid were melted later to form basalts represented by the Apollo 11 Group D and B2 high-Ti mare basalts (Fig. 8). Even later melting (at 3.67–3.71 Ga) included sources with 0.8–1.5% trapped, residual, LMO liquid and generated basalts represented by the Apollo 11 Groups B1–B3 and Apollo 17 Group C basalts (Fig. 8). Based upon limited experimental, pressure-temperature estimates, the sources of these low-K, high-Ti basalts were located at depths of <100 km (Apollo 11 basalts), although possibly as deep as 250 km (one Apollo 17 basalt) (Longhi, 1992). Considering that the average thickness of the Moon's crust is 60 km on the nearside (Mueller et al., 1988), the sources for these high-Ti mare basalts were very shallow in the mantle, consistent with LMO modelling.

Later volcanic activity (~3.59 Ga) at the Apollo 11 and 17 landing sites consists of *high-K*, Group A, high-Ti mare basalts at Apollo 11 and coeval *high-K*, high-Ti pyroclastic volcanism (picritic orange glass, represented by 74220) at both the Apollo 11 and Apollo 17 landing sites. Indeed, high-Ti picritic (orange glass) magmas are thought to be parental to the Apollo 11 Group A, high-Ti mare basalts (Jerde et al., 1994). The evolution of these high-K, high-Ti magmas is distinct from the other low-K, high-Ti basalts in that extensive KREEP assimilation is strongly suggested (Jerde et al., 1994). Furthermore, the high-Ti orange glasses were probably derived from great depth (~500 km; Walker et al., 1975; Longhi, 1992b)

Mare basalts were extruded at the Apollo 15 landing site at 3.4–3.3 Ga ago and were noteably low-Ti in nature. These basalts also were derived from sources at relatively shallow depths, from <100 to 300 km (Longhi, 1992b).

Finally, low-Ti mare basalts at the Apollo 12 landing site were extruded between 3.28 and 3.18 Ga and were derived from upper-mantle, cumulate sources that had even less trapped, residual, LMO liquid (0.15–0.5%) than previous sources (Fig. 8). However, the sources for these basalts lie

at two distinct depths. The olivine and pigeonite basalts were melted from sources located at similarly shallow depths (100–200 km; Longhi, 1992b) as the high-Ti mare basalts from Apollos 11 and 17. In contrast, ilmenite basalts were melted from a source that may have been as deep as 350–400 km. The ilmenite-basalt source is the deepest of the known mare basalt sources, but comparable to other deep sources suggested by studies of high-Ti picritic glass beads (400 to >500 km)(Longhi, 1992). The key feature of these rocks is the presence of signficant amounts of modal ilmenite.

10.2. Ilmenite Sinking in the Mantle: A P-T-t Path

Over time, it is clear that ilmenite-rich mafic magmas (picrites and mare basalts) that would require ilmenite to have been originally in the source can be generated at a variety of depths. However, early on, the ilmenite-bearing melts were solely basaltic and significantly enriched in incompatible elements. This attests to the shallow, more evolved sources for these rocks. With time, these ilmenite-rich melts became less incompatible-element enriched and less evolved, reflecting slightly deeper sources with less trapped KREEPy liquid. Later melting to form ilmenite-bearing basalts and picrites, after a possible hiatus of ~300 million years, was at much greater depths. Yet, trace-element, major-element, and phase modelling indicates that ilmenite was one of the last phases to crystallize from the incipient LMO and, thus, should be found only in the uppermost mantle. Where did these deeper ilmenite-bearing sources come from?

Spera (1992) stated that, due to density contrasts in lunar magma ocean cumulates, ilmenite-bearing layers, formed late in the LMO and precipitated in the uppermost portion of the upper mantle, will sink relative to other cumulates. This was first suggested by Ringwood and Kesson (1976). However, Hess and Parmentier (1993) further projected that most of the ilmenite would continue to sink, eventually forming the lunar core. They also considered it likely that some of this sinking ilmenite would mix with the lunar mantle in transit, thus creating fertile, Ti-enriched source regions throughout the mantle. Combined pressure-temperature information on mare basalts and high-Ti picritic glasses are consistent with such a model. In fact, in may be possible to track the descent of some of these sinking blobs of ilmenite-bearing material by looking at the ages and depths of melting of ilmenite-rich basalts and picrites.

The earliest ilmenite-rich basalts are those found at Apollos 11 and 17 and indicate melting of shallow sources. Sparse age data from high-Ti picritic magmas (as evidenced by picritic glass beads) from these landing sites seem to give younger ages than the mare basalts, in some cases (i.e., Apollo 17) much younger (possibly up to 200 million y younger; Taylor et al., 1991). These high-Ti picritic melts were probably derived from very deep sources (400 to >500 km; Longhi, 1992a). The ilmenite basalts from the Apollo 12 landing site are extruded much later and also come from a very deep source (350–400 km). Thus, extant data suggest that fertile, ilmenite-bearing sources were melted at greater depths over time. This is at least consistent with sinking of the ilmenite-bearing, late LMO, cumulate source over time. An important test of this hypothesis would be the return of samples from the uppermost volcanic units in a broad basin, such as volcanics from the Sharp Formation in Oceanus Procellarum, that are demonstrably younger (2.5 ± 0.5 Ga; Pieters et al., 1980), yet high-Ti in nature. One might suspect that these volcanics would be derived from a very deep source and yield picritic and not basaltic magmas.

The effects of large impacts on basin excavation, fracturing, and regolith formation and insulation undoubtedly contributed to the timing and style of melting of the lunar mantle and magma emplacement. However, the two major controlling factors may prove to be the proportion of trapped, residual, incompatible-element enriched LMO liquid in the cumulate source and the sinking of fertile, ilmenite-bearing material into the lower mantle.

SUMMARY

Volcanism at the Apollo 12 landing site in Oceanus Procellarum occurred over a relatively restricted time interval from 3.18 to 3.20 Ga and produced a diverse group of mare basalts which have been classified previously into three groups—pigeonite, olivine, and ilmenite basalts. Distinct chemical differences occur between the three different groups of Apollo 12 mare basalts. Ilmenite basalts have the highest abundances of the REEs, Y, Zr, Sr, Sc and Hf and the lowest abundances of Rb and Cs. Furthermore, ilmenite basalts are the most LREE depleted of the mare basalts from the Apollo 12 landing site. The initial (at 3.2 Ga) Sr isotopic compositions for these fine-grained basalts define two supergroups, one containing the olivine and pigeonite basalts ($^{87}Sr/^{86}Sr$ = 0.69954–0.69960) and another of ilmenite basalts ($^{87}Sr/^{87}Sr$ = 0.69920–0.69932). Initial Nd isotopic compositions support these two distinct groupings—the ilmenite basalts with ϵ_{Nd} of +10.5 to +11.2 and the pigeonite-olivine-basalt group with ϵ_{Nd} of +4.3 to +4.7.

Trace-element modelling also allows a common source for the fine-grained olivine and pigeonite basalts, athough previous modelling has indicated that their ascent and/or extrusive histories are quite different. Whereas most olivine basalts can be modelled by up to 25% crystal accumulation in magmas which were generated by 5–11% partial melting of the source, pigeonite basalts involved significant assimilation-fractional crystallization with a crustal component (Neal et al., 1994b). Such assimilation for the pigeonite basalts is not seen in our fine-grained parental varieties, consistent with their being parental (i.e., relatively uncontaminated) to the process. Thus, any assimilation must have occurred at the surface during extrusion. Fine-grained parental basalts for both the pigeonite and olivine groups indicate 7–9% partial melting of an olivine-dominated source. The chemical compositions of fine-grained ilmenite basalts 12022 and 12045 are consistent with their derivation by 5–6% nonmodal fractional melting of a source with sub-equal proportions olivine and pigeonite, some clinopyroxene, and a minor entrained plagioclase component.

Chemical modelling of the crystallization of an incipient

lunar magma ocean has allowed us to place constraints on the nature and location of the upper mantle sources for the low-Ti basalts. This modelling included both major and trace-elements exhibiting a range of incompatibilites, including highly incompatible (Rb, Be, LREEs), moderately incompatible (Sr, Li, Hf, HREEs), and compatible (Mg, Fe, Ca, Co). The low-Ti ilmenite basalt source contained $< 0.15\%$, and the olivine-pigeonite basalt source contained from 0.3 to 0.5%, residual magma ocean liquid trapped in the interstices of upper mantle minerals. The low-Ti basalts were melted from sources formed after 82–94% crystallization of an early moon-wide magma ocean, in contrast to high-Ti basalts which were formed from more evolved magma ocean cumulates (after about 95% crystallization; Snyder et al., 1992). It appears that all mare basalts were melted from the uppermost 20% of the magma ocean cumulate pile.

Finally, we have proposed a model for melting of the lunar interior over time which includes

1) formation of cumulate source-regions with variable proportions of trapped, residual LMO liquid (the proportion likely decreasing with depth);
2) early melting of those source regions that are shallow, the most fertile, and that have the highest proportions of trapped LMO liquid (and thus the highest incompatible-element abundances and the greatest amount of heat-producing elements) — these sources happen to have significant ilmenite in the mineral assemblage and generate high-Ti mare basalts;
3) later melting of progressively deeper sources with smaller proportions of trapped LMO liquid; and
4) sinking of the ilmenite-bearing upper layers of the mantle into the lower mantle carrying more fertile source material and allowing the melting of more Mg-enriched magmas (represented by picritic glass beads).

Acknowledgments— We greatly appreciate the insightful reviews of John Delano, Larry Nyquist, and Graham Ryder, and the editorial handling of executive editor Karl Turekian. This research was supported by NASA grants NAGW 9-62 and NAGW 9-415 (to L.A.T.), NSF grants 90-04133, 91-04877, and 92-05435 (to A.N.H.), and NSF grant ECS 92-14596 (to C.R.N.).

REFERENCES

Alexander E. C., Jr. and Davis P. K. (1974) ^{40}Ar-^{39}Ar ages and trace element contents of Apollo 14 breccias: An interlaboratory cross-calibration of ^{40}Ar-^{39}Ar standards. *Geochim. Cosmochim. Acta* **38**, 911–928.

Baldridge W. S., Beaty D. W., Hill S. M. R., and Albee A. L. (1979) The petrology of the Apollo 12 pigeonite basalt suite. *Proc. Lunar Planet. Sci. Conf.* **10**, 141–179.

Beard B. L., Snyder G. A., and Taylor L. A. (1994) Deep melting and residual garnet in the sources of lunar basalts: Lu-Hf isotopic systematics. *Lunar Planet. Sci.* **XXV**, 73–74 (extended abstr).

Beard B. L., Taylor L. A., Scherer E. E., Johnson C. M., and Snyder G. A. (1996) The source mineralogy of high- and low-Ti basalts based on their Hf isotopic composition. *Lunar Planet. Sci.* **XXVII**, 81–82 (extended abstr).

Beaty D. W., Hill S. M. R., Albee A. L., and Baldridge W. S. (1979) Apollo 12 feldspathic basalts 12031, 12038, and 12072: Petrology, comparison and interpretations. *Proc. Lunar Planet. Sci. Conf.* **10**, 115–139.

Compston W., Berry H., Vernon M. J., Chappell B. W., and Kaye M. J. (1971) Rubidium-strontium chronology and chemistry of lunar material from the Ocean of Storms. *Proc. Lunar Sci. Conf.* **2**, 1471–1485.

Cuttitta F. et al. (1971) Elemental composition of some Apollo 12 lunar rocks and soils. *Proc. Lunar Sci. Conf.* **2**, 1217–1229.

Delano J. W. (1986) Pristine lunar glasses: Criteria, data, and implications. *Proc. Lunar Planet. Sci. Conf.* **16**, D201–D213.

DePaolo[au:supply initial(s)] and Wasserburg[au:supply initial(s)] (1976) Nd isotopic variations and petrogenetic models. *Geophys. Res. Lett.* **3**, 249–252.

Dreibus G., Spettel B., and Wänke H. (1976) Lithium as a correlated element, its condensation behavior, and its use to estimate the bulk composition of the Moon and the eucrite parent body. *Proc. Lunar Sci. Conf.* **7**, 3383–3396.

Dungan M. A. and Brown R. W. (1977) The petrology of the Apollo 12 ilmenite basalt suite. *Proc. Lunar Sci. Conf.* **8**, 1339–1381.

Engel A. E. J., Engel C. G., Sutton A. L., and Myers A. T. (1971) Composition of five Apollo 11 and Apollo 12 rocks and one Apollo 11 soil and some petrogenic considerations. *Proc. Second Lunar Sci. Conf.* **2**, 439–448.

Green D. H., Ringwood A. E., Ware N. G., Hibberson W. O., Major A., and Kiss E. (1971a) Experimental petrology and petrogenesis of Apollo 12 basalts. *Proc. 2nd Lunar Sci. Conf.* **2**, 601–615.

Green D. H., Ware N. G., Hibberson W. O., Major A. (1971b) Experimental petrology of Apollo 12 basalts: Part 1, sample 12009. *Earth Planet. Sci. Lett.* **13**, 85–96.

Head J. W. and Wilson L. (1992) Lunar mare volcanism: Stratigraphy, eruption conditions, and the evolution of secondary crusts. *Geochim. Cosmochim. Acta* **56**, 2155–2175.

Hess P. C. (1993) The ilmenite liquidus and depths of segregation for high-Ti picrite glasses . *Lunar Planet. Sci.* **XXIV**, 649–650 (extended abstr).

Hess P. C. and Parmentier E. M. (1993) Overturn of magma ocean ilmenite cumulate layer: Implications for lunar magmatic evolution and formation of a lunar core. *Lunar Planet. Sci.* **XXIV**, 651–652 (extended abstr).

Hess P. C. and Parmentier E. M. (1995) A model for thermaland chemical evolution of the Moon's interior: Implications for the onset of mare volcanism. *Earth Planet. Sci. Lett.* **134**, 501–514 (extended abstr).

Horn P., Jessberger E. K., Kirsten T., and Richter H. (1975) ^{39}Ar-^{40}Ar dating of lunar rocks: Effects of grain size and neutron irradiation. *Proc. Lunar Sci. Conf.* **6**, 1563–1591.

Hughes S. S., Delano J. W., Schmitt R. A. (1988) Apollo 15 yellow-brown glass: Chemistry and petrogenetic relations to green volcanic glass and olivine-normative mare basalts. *Geochim. Cosmochim. Acta* **52**, 2379–2391.

Hughes S. S., Delano J. W., and Schmitt R. A. (1989) Petrogenetic modeling of 74220 high-Ti orange volcanic glasses and the Apollo 11 and 17 high-Ti mare basalts. *Proc. Lunar Planet. Sci. Conf.* **19**, 175–188.

James O.B. and Wright T. L. (1972) Apollo 11 and 12 mare basalts and gabbros: classification, compositional variations, and possible petrogenetic relations. *Geol. Soc. Amer. Bull.* **83**, 2357–2382.

Jerde E. A., Snyder G. A., Taylor L. A., Liu Y.-G., and Schmitt R. A. (1994) The origin and evolution of lunar high-Ti basalts: Periodic melting of a single source at Mare Tranquillitatis. *Geochim. Cosmochim. Acta* **58**, 515–527.

Kushiro I., Nakamura Y., Kitayama K., and Akimoto S. (1971) Petrology of some Apollo 12 crystalline rocks. *Proc. Lunar Sci. Conf.* **2**, 481–495. Kuskov O. L. (1995) Constitution of the Moon: 3. Composition of middle mantle from seismic data. *Phys. Earth Planet. Int.* **90**, 55–74.

Longhi, J. (1987) On the connection between mare basalts and picritic volcanic glasses. *Proc. Lunar Planet. Sci. Conf.* **17**, E349–E360.

Longhi J. (1992a) Origin of picritic green glass magmas by polybaric fractional fusion. *Proc. Lunar Planet. Sci.* **22**, 343–353.

Longhi J. (1992b) Experimental petrology and petrogenesis of mare volcanics. *Geochim. Cosmochim. Acta* **56**, 2235–2251.

Marsh B. D. and Maxey M. R. (1985) On the distribution and separation of crystals in convecting magma. *J. Volc. Geotherm. Res.* **24**, 95–150.

McDonough W. F., Sun S. -S., Ringwood A. E., Jagoutz E., and Hofmann A. W. (1992) Potassium, rubidium, and cesium in the Earth and Moon and the evolution of the mantle of the Earth. *Geochim. Cosmochim. Acta* **56**, 1001–1012.

Mueller S., Taylor G. J., Phillips R. J. (1988) Lunar composition: A geophysical and petrological synthesis. *J. Geophys. Res.* **93**, 6338–6352.

Murthy V. R., Evensen N. M., Jahn B. M., and Coscio M. R., Jr. (1971) Rb-Sr ages and elemental abundances of K, Rb, Sr, and Ba in samples from the Ocean of Storms. *Geochim. Cosmochim. Acta* **35**, 1139–1153.

Nakamura Y. (1983) Seismic velocity structure of the lunar mantle. *J. Geophys. Res.* **88**, 677–686.

Neal C. R. and Taylor L. A. (1992) Petrogenesis of mare basalts: A record of lunar volcanism. *Geochim. Cosmochim. Acta* **56**, 2177–2211.

Neal C. R., Hacker M. D., Snyder G. A., Taylor L. A., Liu Y.-G., and Schmitt R. A. (1994a) Basalt generation at the Apollo 12 site, Part 1: New data, classification, and re-evaluation. *Meteoritics* **29**, 334–348.

Neal C. R., Hacker M. D., Snyder G. A., Taylor L. A., Liu Y.-G., and Schmitt R. A. (1994b) Basalt generation at the Apollo 12 site, Part 2: Source heterogeneity, multiple melts, and crustal contamination. *Meteoritics* **29**, 349–361.

Norman M. D. and Taylor S. R. (1992) Geochemistry of lunar crustal rocks from breccia 67016 and the composition of the Moon. *Geochim. Cosmochim. Acta* **56**, 1013–1024.

Nyquist L. E. and Shih C.-Y. (1992) On the chronology and isotopic record of lunar basaltic volcanism. *Geochim. Cosmchim. Acta* **56**, 2213–2234.

Nyquist L. E., Hubbard N. J., Gast P. W., Bansal B. M., Wiesmann H., and Jahn B. (1973) Rb-Sr systematics for chemically defined Apollo 15 and 16 materials. *Proc. Lunar Sci. Conf.* **4**, 1823–1846.

Nyquist L. E., Bansal B. M., Wooden J. L., and Wiesmann H. (1977) Sr-isotopic constraints on the petrogenesis of Apollo 12 mare basalts. *Proc. Lunar Sci. Conf.* **8**, 1383–1415.

Nyquist L. E., Shih C.-Y., Wooden J. L., Bansal B. M., and Wiesmann H. (1979) The Sr and Nd isotopic record of Apollo 12 basalts: Implications for lunar geochemical evolution. *Proc. Lunar Planet. Sci. Conf.* **10**, 77–114.

Nyquist L. E., Wooden J. L., Shih C.-Y., Wiesmann H., and Bansal B.M. (1981) Isotopic and REE studies of lunar basalt 12038: Implications for petrogenesis of aluminous mare basalts. *Earth Planet. Sci. Lett.* **55**, 335–355.

Nyquist L. E., Wiesmann H., Bansal B., Shih,C.-Y., Keith J. E., and Harper C. L. (1995) ^{146}Sm-^{142}Nd formation interval for the lunar mantle. *Geochim. Cosmochim. Acta* **59**, 2817–2837.

O'Neill H. St.C. (1991) The origin of the Moon and the early history of the Earth—a chemical model. Part 1: The Moon. *Geochim. Cosmochim. Acta* **55**, 1135–1157.

Papanastassiou D. A. and Wasserburg G. W. (1970) Rb-Sr ages from the Ocean of Storms. *Earth Planet. Sci. Lett.* **8**, 269–278.

Papanastassiou D. A. and Wasserburg G. W. (1971a) Lunar chronology and evolution from Rb-Sr studies of Apollo 11 and 12 samples. *Earth Planet. Sci. Lett.* **11**, 37–62.

Papanastassiou D. A. and Wasserburg G. W. (1971b) Rb-Sr ages of igneous rocks from the Apollo 14 mission and the age of the Fra Mauro formation. *Earth Planet. Sci. Lett.* **12**, 36–48.

Papanastassiou D. A., DePaolo D. J., and Wasserburg G. J. (1977) Rb-Sr and Sm-Nd chronology and genealogy of mare basalts from the Sea of Tranquillity. *Proc. Lunar Sci. Conf.* **8**, 1639–1672.

Pieters C. M., Head J. W., Adams J. B., McCord T. B., Zisk S. H., and Whitford-Stark J. L. (1980) Late high-Ti basalts of the western maria: Geology of the Flamsteed region of Oceanus Procellarum. *J. Geophys. Res.* **85**, 3913–3938.

Rhodes J. M., Blanchard D. P., Dungan M. A., Brannon J. C., and Rodgers K. V. (1977) Chemistry of Apollo 12 mare basalts: Magma types and fractionation processes. *Proc. Lunar Sci. Conf.* **8**, 1305–1338.

Ringwood A. E. (1992) Volatile and siderophile element geochemistry of the Moon: A reappraisal. *Earth Planet. Sci. Lett.* **111**, 537–555.

Ringwood A. E. and Kesson S. E. (1976) A dynamic model for mare basalt petrogenesis. *Proc. Lunar Sci. Conf.* **7**, 1697–1722.

Ryan J. G. and Langmuir C. H. (1987) The systematics of lithium abundances in young volcanic rocks. *Geochim. Cosmochim. Acta* **51**, 1727–1741.

Ryan J. G. and Langmuir C. H. (1988) Beryllium systematics in young volcanic rocks: Implications for ^{10}Be. *Geochim. Cosmochim. Acta* **52**, 237–244.

Ryan J. G. and Langmuir C. H. (1993) The systematics of boron abundances in young volcanic rocks. *Geochim. Cosmochim. Acta* **57**, 1489–1498.

Ryder G. (1987) Petrographic evidence for nonlinear cooling rates and a volcanic origin for Apollo 15 KREEP basalts. *Proc. Lunar Planet. Sci. Conf.* **17**, E331–E339.

Ryder G. (1991) Lunar ferroan anorthosites and mare basalt sources: The mixed connection. *Geophys. Res. Lett.* **18**, 2065–2068.

Ryder G. (1994) Coincidence in time of the Imbrium basin impact and Apollo 15 KREEP volcanic flows: The case for impact-induced melting. In *Large Meteorite Impacts and* Planetary Evolution, (eds. B. O. Dressler et al.); *Geol. Soc. America Spec. Paper* **293**, 11–18.

Schnetzler C. C. and Philpotts J. A. (1971) Alkali, alkaline earth, and rare-earth element concentration in some Apollo 12 soils, rocks, and separated phases. *Proc. Lunar Sci. Conf.*, **2**, 1101–1122.

Shearer C. K. and Papike J. J. (1993) Basaltic magmatism on the Moon: A perspective from volcanic picritic glass beads. *Geochim. Cosmochim. Acta* **57**, 4785–4812.

Shearer C. K., Layne G. D., and Papike J. J. (1994) The systematics of light lithophile elements (Li, Be, and B) in lunar picritic glasses: Implications for basaltic magmatism on the Moon and the origin of the Moon. *Geochim. Cosmochim. Acta* **58**, 5349–5362.

Shearer C. K., Papike J. J., and Layne G. D. (1996) The role of ilmenite in the source region for mare basalts: Evidence from niobium, zirconium, and cerium in picritic glasses. *Geochim. Cosmochim. Acta* **60**, 3521–3530.

Shih C.-Y. and Schonfeld E. (1976) Mare basalt genesis: A cumulate-remelting model. *Proc. Lunar Sci. Conf.* **7**, 1757–1792.

Shih C.-Y., Nyquist L. E., Bansal B. M., and Wiesmann H. (1992) Rb-Sr and Sm-Nd chronology of an Apollo 17 KREEP basalt. *Earth Planet. Sci. Lett.* **108**, 203–215.

Snyder G. A. and Taylor L. A. (1993) Constraints on the genesis and evolution of the Moon's magma ocean and derivative cumulate sources as supported by lunar meteorites. *Proc. NIPR Symp. Antarctic Met.* **6**, 246–267.

Snyder G. A., Taylor L. A., and Neal C. R. (1992) A chemical model for generating the sources of mare basalts: Combined equilibrium and fractional crystallization of the lunar magmasphere. *Geochim. Cosmochim. Acta* **56**, 3809–3823.

Snyder G. A., Lee D.-C., Taylor L. A., Halliday A. N., and Jerde E. A. (1994) Evolution of the upper mantle of the Earth's Moon: Neodymium and strontium isotopic constraints from high-Ti mare basalts. *Geochim. Cosmochim. Acta* **58**, 4795–4808.

Snyder G. A., Hall C. M., Lee D.-C., Taylor, L. A., and Halliday, A.N. (1996) Earliest high-Ti volcanism on the Moon: ^{40}Ar-^{39}Ar, Sm-Nd, and Rb-Sr isotopic studies of Group D basalts from the Apollo 11 landing site. *Meteor. Planet. Sci.* **31**, 328–334.

Snyder G. A., Lee D. C., Taylor L. A., and Halliday A. N. (1997) Earliest lunar volcanism: An alternative interpretation of the Apollo 14 high-Al basalts from Nd-Sr-Hf isotopic studies. *Meteor. Planet. Sci.* (submitted).

Spera F. J. (1992) Lunar magma transport phenomena. *Geochim. Cosmochim. Acta* **56**, 2253–2265.

Stettler A., Eberhardt P., Geiss J., Grogler N., and Maurer P. (1973)

Ar^{39}-Ar^{40} ages and Ar^{37}-Ar^{38} exposure ages of lunar rocks. *Proc. Lunar Sci. Conf.* **4**, 1865–1888.

Taylor G. J., Warren P. H., Ryder G., Delano J., Pieters C., and Lofgren G. (1991) Lunar rocks. In *Lunar Sourcebook: A User's Guide to the Moon* (eds. G. H. Heiken et al.), pp.183–284. Cambridge Univ. Press.

Taylor L. A. and Lu F. (1992) The formation of ore mineral deposits on the Moon: A feasibility study. In *The Second Conference on Lunar Bases and Space Activities of the 21st Century*([ed])NASA Publ. **2**, 379–383.

Taylor S. R. (1982) *Planetary Science: A Lunar Perspective.* Lunar Planetary. Institute.

Turner G. (1971) ^{40}Ar-^{39}Ar ages from the lunar maria. *Earth Planet. Sci. Lett.* 11, 169–191.

Unruh D. M., Stille P., Patchett P. J., Tatsumoto M. (1984) Lu-Hf and Sm-Nd evolution in lunar mare basalts. *Proc. Lunar Planet. Sci. Conf.* **14**, B459–B477.

Walker D., Longhi J., Stolper E. M., Grove T., and Hays J. F. (1975) Origin of titaniferous lunar basalts. *Geochim. Cosmochim. Acta* **39**, 1219–1235.

Walker D., Kirkpatrick R. J., Longhi J., and Hays J. F. (1976) Crystallization history of lunar picritic basalt sample 12002: Phase equilibria and cooling rate studies. *Geol. Soc. Amer. Bull.* **87**, 646–656.

Wänke H.et al.. (1971) Apollo 12 samples: Chemical composition and its relation to sample locations and exposure ages, the two component origin of various soil samples and studies on lunar metallic particles. *Proc. Lunar Sci. Conf.* **2**, 117–1208.

Warner J. L. (1971) Lunar crystalline rocks: Petrology and geology. *Proc Lunar Sci. Conf.* **2**, 469–480.

Warren P. H. (1985) The lunar magma ocean concept and lunar evolution. *Ann. Rev. Earth Planet. Sci.* **13**, 201–240.

Wasson J. T. and Kallemeyn G. W. (1988) Compositions of chondrites. *Phil. Transactions Royal Soc. London.* **A 325**, 535–544.

Whitford-Stark J. L. and Head J. W. (1980) Stratigraphy of Oceanus Procellarum basalts: Sources and styles of emplacement. *J. Geophys. Res.* **85**, 6579–6609.

Wilhelms D. E. (1987) The Geologic History of the Moon. *U.S. Geol. Surv. Prof. Paper 1348.*